Influence of non-equilibrium and nonlinear sorption of 137Cs in soils. Study with stirred flow-through reactor experiments and quantification with a nonlinear equilibrium-kinetic model

Hamza Chaif, Arnaud Martin-Garin, Sylvie Pierrisnard, Daniel Orjollet, Vanessa Tormos, Laurent Garcia-Sanchez

Influence of non-equilibrium and nonlinear sorption of ^{137}Cs in soils. Study with stirred flow-through reactor experiments and quantification with a nonlinear equilibrium-kinetic model.

Hamza Chaif[(a)], Arnaud Martin-Garin[(a)], Sylvie Pierrisnard[(a)], Daniel Orjollet[(a)], Vanessa Tormos [(a)] and Laurent Garcia-Sanchez[(a)*]

[(a)] : *Institute of Radiological Protection and Nuclear Safety (IRSN), Laboratory of Research on Radionuclide Transfers in Terrestrial Ecosystems (LR2T), CE Cadarache, 13115, Saint-Paul-lez-Durance Cedex, France.*

***** *Corresponding author: laurent.garcia-sanchez@irsn.fr*

ABSTRACT

This paper addresses the modelling of cesium sorption in non-equilibrium and nonlinear conditions with a two-site model. Compared to the classical K_d approach, the proposed model better reproduced the breakthrough curves observed during continuous-flow stirred tank reactor experiments conducted on two contrasted soils. Fitted parameters suggested contrasted conditions of cesium sorption between 1) equilibrium sites, with low affinity and high sorption capacity comparable to CEC and 2) non-equilibrium sites, with a fast sorption rate (half-time of 0.2-0.3 hours), a slow desorption rate (half-time of 3-9 days) and a very low sorption capacity (0.02-0.04% of CEC). Comparison of EK sites densities with sorption capacities derived from the literature suggests that the EK equilibrium and kinetic sites might correspond to ion exchange and surface complexation of soil clay minerals respectively. This work stresses the limits of the K_d model to predict ^{137}Cs sorption in reactive transport conditions and supports an alternative non-equilibrium nonlinear approach.

KEYWORDS

cesium; sorption; soil; modelling; experiment; inverse modelling

1. INTRODUCTION

The various processes of solute retention on solid phases –referred to as *sorption* (Sposito, 1984)– strongly govern the mobility, bioavailability and remediation of substances in the environment, and, in the case of radioactive substances, their radiological impact. They notably control the conditions of reactive transport of solutes occurring in solid-liquid systems such as rivers, soils and groundwater (Bouzidi et al., 2010; Fiengo Perez et al., 2015; Ilina et al., 2020; Limousin et al., 2007). A critical issue when assessing the reactive transport of solutes (such as radionuclides) in solid-liquid systems such as soils concerns the hypotheses and parameters modelling the rate of solute transfer between the solution and solid phases (Ardois and Szenknect, 2005; Chaif et al., 2021; Cherif et al., 2017; Limousin et al., 2007).

In impact assessment models, sorption is most commonly represented for a wide range of contaminants (including radionuclides) by an instantaneous, concentration-independent and completely reversible reaction, using an equilibrium coefficient also called distribution coefficient and noted K_d (IAEA, 2009). This model simply assumes a constant proportion (K_d) between concentrations in sorbed and soluble phases and, as a result, a constant proportion (called retardation factor) between water and solute fluxes (Bossew and Kirchner, 2004; Mishra et al., 2018; Szenknect et al., 2003). However, the K_d sorption model is not fully predictive. Deviations from its simplifying hypotheses have been reported for many solutes (including pesticides, radionuclides and notably cesium-137) and may result notably in earlier

47 solute arrival in groundwater and longer residence time in soils than the ideal K_d model (Bahr
48 and Rubin, 1987; Schnaar and Brusseau, 2014). These deviations essentially result from:

49 1) Chemical non-equilibrium: sorption sites may differ in their reactivity with the solute,
50 some reacting instantaneously and other slower than contact times with water (Chaif et al.,
51 2021; Kurikami et al., 2017; Ota et al., 2016; Sardin et al., 1991). Important special cases are
52 sorption irreversibility or pseudo-irreversibility: for a fraction of adsorbed solutes, the
53 remobilization back into solution may be impossible or so slow that it can be considered as
54 irreversible (Antonopoulos-Domis et al., 1995; Comans and Hockley, 1992; Montes et al.,
55 2013; Toso and Velasco, 2001).

56 2) Physical non-equilibrium: some sorption sites may not be instantaneously accessible to
57 the solute but limited by physical processes such as external and internal diffusion in solid
58 particles (Chen et al., 2020; van Genuchten and Wagenet, 1989).

59 3) Sorption nonlinearity: sorption may vary with solute concentration if it involves
60 multiple sorption sites having different densities and affinities for solute. For instance,
61 sorption can be high at trace levels when selective sorption sites are concerned, and much
62 lower when non-selective sorption sites also participate to solid-liquid exchanges (Cherif et
63 al., 2017; Fesch et al., 1998; Wang et al., 1998).

64 For a better description of sorption, various multi-site equilibrium and/or kinetic (EK)
65 models have been proposed. These empirical models, initially introduced for agrochemicals
66 and heavy metals (Cameron and Klute, 1977; Selim and Mansell, 1976; van Genuchten and
67 Wagenet, 1989), mitigate the K_d hypotheses by assuming that sorption occurs on 2–3 different
68 types of solid sites, governed by equilibrium and/or kinetic rates. Depending on the modelled
69 solutes, the existing variants combine multiple sorption properties such as equilibrium (e.g.
70 linear isotherm), non-equilibrium (first order, second order sorption rates), non-linearity (e.g.

71 Langmuir, Freundlich isotherms) and sorption irreversibility. More recently, promising
72 applications of EK models for radionuclide have been reported (Antonopoulos-Domis et al.,
73 1995; Chaif et al., 2021; Garcia-Sanchez et al., 2014; Ota et al., 2016; Toso and Velasco,
74 2001; Wang et al., 1998). However, the benefits of adopting equilibrium kinetic models of
75 sorption have not been fully demonstrated. The process-based validation of these approaches
76 still requires the interpretation of the different types of sorption sites in terms of real
77 contamination pools and not hidden virtual compartments. Moreover, the scenarios of reactive
78 transport for which EK hypotheses significantly improve the realism of predictions, compared
79 to the simple K_d hypotheses, must be clarified.

80 Sorption reactions in soils have been studied both in the laboratory and in the field by
81 complementary experimental devices that achieve different levels of representativity and
82 bring different levels of information about sorption reactions. They usually consist in batch
83 experiments that allow a static study of sorption reactions in solid suspensions, or soil column
84 experiments that allow the study of reactive transport in porous media.

85 An intermediate experimental device known as *stirred flow-through reactor experiments*,
86 or continuous-flow stirred-tank reactor (CSTR) experiments, is particularly adapted to the
87 study of rate-limited sorption under flowing conditions in disperse solid phases. This device
88 consists in a well-mixed stirred cell, containing a known mass of solid and a known volume of
89 solution (e.g. Garcia-Sanchez et al., 2014; Martin-Garin et al., 2003; Sparks et al., 1980; Van
90 Cappellen and Qiu, 1997a,b) (**Figure 1**). During a classical reactor experiment, the injection
91 flowrate is generally held constant (Q_i) and the injected solute concentration consists in a
92 finite step function (with value C_i), while the dissolved concentration (C_w) is monitored at the
93 reactor outlet (**Figure 2**). Different reactor conditions allow then to test experimentally if
94 solute reactions depend on solute-concentration (C_i) and flowrate (Q), and are thus nonlinear
95 and not instantaneous (Bar-Tal et al., 1990).

All these protocols require an inverse approach consisting in selecting a sorption model and estimating its parameters from observations by frequentist or bayesian calibration (e.g. Nicoulaud-Gouin et al., 2016; Toro and Padilla, 2017; van Genuchten et al., 2012). For model selection, varying contact times and influent concentrations have been recommended to test linearity and equilibrium hypotheses and reject improper models (e.g. Bar-Tal et al., 1990; Nicoulaud-Gouin et al., 2016). For parameter identification, the unicity of the sorption parameters derived from observations, also termed identifiability, must also be examined attentively to ensure that obtained parameter values are physically interpretable (Belsley et al., 1980; Brun et al., 2001; Stewart, 1987).

Large amounts of radionuclide have been released in the environment after the multiple nuclear weapons tests that took place from the 1950s to 1980 and the nuclear accidents of Chernobyl (1986) and Fukushima (2011) (Castrillejo et al., 2016; Klement, 1965; Steinhauser et al., 2015). Among these elements, ^{137}Cs – due to its relatively long half-life ($t_{1/2}$ = 30.2 years) – is considered the main source of radioactive soil contamination (Avery, 1996; Strebl et al., 1999) and the first source of nuclear waste in the first one hundred years after release.

Cesium sorption in soils is primarily governed by clay minerals (Bostick et al., 2002; Chorover et al., 2003; Missana et al., 2014a; Savoye et al., 2012; Shenber and Eriksson, 1993; Wendling et al., 2005). In fact, radiocesium sorbs strongly and specifically on clay minerals (Cornell, 1993; Fuller et al., 2015; Okumura et al., 2019) but also less intensely on iron oxides and organic matter which often represent large sorption capacities (Rigol et al., 2002; Schwertmann and Taylor, 1989). On clay minerals, surface adsorption sites are very heterogeneous (Bradbury and Baeyens, 2000; Cornell, 1993; Eliason, 1966; Missana et al., 2004; Poinssot et al., 1999; Staunton and Roubaud, 1997; Wahlberg and Fishman, 1962). Five types of sorption sites are generally distinguished: basal surface sites, edge sites, hydrated interlayer sites, frayed edge sites (FES), and interlayer sites (Okumura et al., 2019). These

sites have contrasted densities and affinities to cesium. Hydrated interlayer, FES, and interlayer sites (that can be grouped under the term "interlayer sites") have strong affinity to cesium but low density (Brouwer et al., 1983; Eberl, 1980; Francis and Brinkley, 1976; Jackson, 1962; Maes and Cremers, 1986; Poinssot et al., 1999; Rich and Black, 1964; Sawhney, 1972; Zachara et al., 2002). Planar sites have much lower affinity to cesium but represent most of the cation exchange capacity "CEC" and correspond to the basal surface and edge sites (Cornell, 1993; Rigol et al., 2002; Staunton and Roubaud, 1997; Zachara et al., 2002). Numerous laboratory studies indicate that Cs sorption is both time-dependent and concentration-dependent. Sorption experiments show that, although 137Cs sorption is initially rapid (minutes), it continues for months from non-selective to highly selective sorption sites (Konoplev et al., 1997). Desorption experiments also indicate that desorption of 137Cs is very slow (e.g. ~2 years of half-life for Fukushima soils reported by Murota et al., 2016) particularly on clay minerals (Durrant et al., 2018). Moreover, many sorption isotherms indicate that affinity to cesium decrease when the concentration of soluble cesium (Cs+) and its competitors (mainly K+) increase in solution (Cherif, 2017; Siroux, 2017).

This work aimed at studying the hypotheses of non-equilibrium and non-linearity of cesium sorption in reactive transport conditions. Our specific objectives were to: (1) quantify the influence of cesium concentration and water transit time on sorption, (2) propose a simple sorption model taking into account these effects, (3) study the validity of this model and estimate its parameters, (4) relate the model compartments and parameters to measurable soil properties. For these purposes, flow-through reactor experiments were conducted on two contrasted soils under different conditions of injection concentration and flow rate. A 5-parameter equilibrium-kinetic model (EK5) including both sorption non-equilibrium and non-linearity was proposed to model cesium sorption and compared to a classical K_d approach. A

145 nonlinear regression approach was adopted to estimate K_d and EK5 parameters and to test
146 EK5 vs K_d hypotheses.

2. MATERIAL AND METHODS

2.1. Studied Soils

Two soils, noted "Soil H" and "Soil S", were selected for their contrasted physico-chemical and mineralogical properties (**Table 1**). Soil S was a calcareous sandy soil with pH = 9.32, 1.44‰ of organic matter, and CEC= 1.11 cmol+/kg. Soil H, on the other hand, had a loamy texture with pH = 5.5, 49.4‰ of organic matter, and CEC = 7.64 cmol+/kg. Soil samples were air dried and sieved (<2 mm) before use. For soil S, mineralogy of the fraction below 2µm was determined by ERM laboratory (Poitiers, France) using powder X-ray diffractometer (Bruker D8 Advance A25) with CuKα radiation at 40kV and 40 mA on oriented mounts. The same technique was used for soil H and the results were already published in a previous study (Siroux, 2017; Siroux et al., 2021). The detailed mineral composition of soils H and S is given in **Table S1** (in supplementary materials).

160

161 **Table 1.** Physico-chemical and mineralogical characteristics of soils H and S. Clay, silt and
162 sand percentages correspond to the granulometric classes of the international scale. Illite,
163 montmorillonite and kaolinite percentages correspond to mineralogical composition of the
164 fraction of the soils below 2 µm, as determined by the X-Ray Diffractometry (XRD)
165 technique. Percentage intervals correspond to the range of realistic mineralogical
166 compositions compatible with the analytical results.

	Soil H*	**Soil S**
Clay (%)	13.13	3.10
Silt (%)	54.05	0.70
Sand (%)	32.82	96.20
pH (H_2O)	5.5	9.3
Organic matter (g/kg)	49.40	1.44
N (g/kg)	2.64	0.04
$CaCO_3$ (g/kg)	14	118
Exchangeable cations (cmol+/kg)		
CEC	7.64	1.11
CEC <2µm	20.0	18.7
K^+	0.32	0.23
Na^+	0.20	0.14
Ca^{2+}	3.23	31.20
Mg^{2+}	0.60	0.72
Mineralogy		
Illite (%)	11 - 22	0 - 2

Montmorillonite (%)	43 - 56	23 - 27
Kaolinite (%)	14 - 23	4 - 9

167 * data from Siroux (2017)

168

2.2. Stirred flow-through reactor experiments

Principles of continuous-flow stirred tank reactor experiments are presented in introduction. Each experiment consisted in injecting an input solution into a chamber of volume V_r containing a known mass of soil m, and measuring ^{137}Cs concentration (C_w) at the output port of the chamber (Garcia-Sanchez et al., 2014; Martin-Garin et al., 2003; Van Cappellen and Qiu, 1997a,b) (**Figure 1**). The input and output ports were equipped with 0.45 µm pore size hydrofoil Teflon membranes (HVLP, Millipore). The input solution was injected at a constant flow rate in the reactor cell by a chromatography system (ÄKTA^{TM} pure 25), and the direction of the flow was periodically reversed to avoid filter clogging. The continuous stirring was ensured by attaching the reactor to an external shaker. This method was preferred to a magnetic stir bar inside the cell to avoid destroying the solid particles. Samples were collected using a fraction collector and analyzed for ^{137}Cs activity using a pure germanium gamma spectrometer (Camberra EGPC 42.190.R).

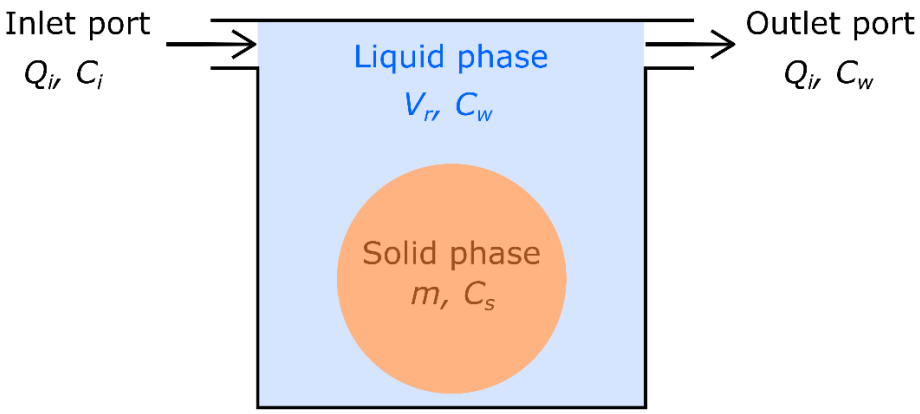

Figure 1. Principle of the continuous-flow stirred tank reactor (CSTR) experiments conducted in this study. A solution is injected into the reactor chamber (of volume V_r) by its inlet port.

187 The solution is injected at a constant flow rate Q_i and is only contaminated during
188 contamination stage (with concentration C_i). Contaminant dilutes and interacts with the solid
189 phase (with mass m and contamination concentration C_s) inside the chamber. The reactor
190 chamber is well-mixed and has a homogenous contaminant concentration in solution C_w that
191 is monitored at the outlet port.

192

193 Each experiment consisted in a constant injection flow rate with three stages of
194 contaminant injection (**Figure 2**): (1) a pre-contamination stage (noted stage I) during which a
195 cesium-free solution was injected for at least 48 hours to allow the soil particles to reach a
196 chemical equilibrium with the input solution; (2) A contamination stage (noted stage II),
197 during which a cesium solution at a known concentration (C_i) was injected until the
198 normalized cesium concentration C_w/C_i either stabilized or reached 1; (3) A decontamination
199 stage (noted stage III) during which the cesium-free solution was again injected until the
200 normalized cesium concentration (C_w/C_i) was below 4%.

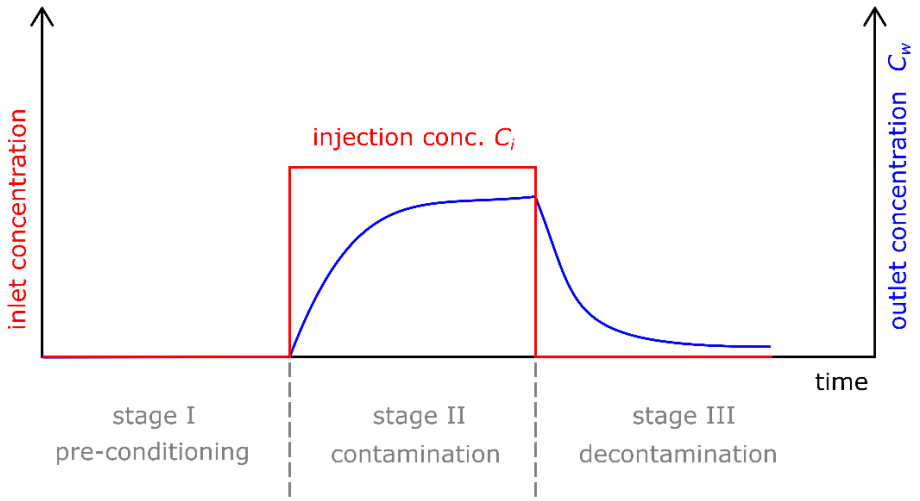

Figure 2. The three stages of continuous-flow stirred tank reactor (CSTR) experiments conducted in this study. During each experiment, input solution was injected at a constant flow rate Q_i (mL h^{-1}). During pre-conditioning (I) and decontamination (III) stages, input solution was a cesium-free solution. During contamination (II), input solution had a constant cesium concentration C_i (mol L^{-1}).

2.3. Input solutions

Cesium-free input solutions (**Table 2**) were designed to mimic the soil solution in equilibrium with the soil. They were injected during the stages I and III of the experiments. For soil S, Ultrapure water (18 MΩ resistivity) was equilibrated with excessive amounts of calcite ($CaCO_3$) and agitated in an open recipient to allow equilibrium with ambient air for at least 15 days. The solution was then filtered and spiked with sodium chloride. For soil H, Ultrapure pure water was directly spiked by a mixture of sodium chloride (NaCl), calcium chloride ($CaCl_2$), calcium nitrate ($Ca(NO_3)_2$) and potassium chloride (KCl).

217 Cesium input solutions were prepared by spiking cesium-free input solutions with
218 approximate cesium concentrations of 10^{-3} mol L^{-1}, 10^{-5} mol L^{-1}, and 10^{-8} mol L^{-1} depending
219 on the experiments (**Table 3**). These contaminated solutions were injected during the stages II
220 of the experiments. This spiking was achieved by adding a mixture of stable (CsCl) and
221 radioactive (^{137}Cs) cesium and then solution pH was adjusted (to pH=8.3 and 5.1 for soils S
222 and H, respectively) by adding a sodium hydroxide solution (NaOH). All cesium input
223 solutions contained approximately 500 Bq mL^{-1} of ^{137}Cs.

224

225 **Table 2.** Composition of the input solutions used for the stirred flow-through reactor
226 experiments with the soils S and H. All concentrations are presented in mol L^{-1}

Property	Soil S	Soil H
$[Ca^{2+}]$	5.00E-04	3.00E-04
$[Na^{+}]$	5.00E-03	1.40E-04
$[Cl^{-}]$	5.00E-03	3.43E-04
$[NO^{3-}]$	-	4.60E-04
$[K^{+}]$	-	6.30E-05
pH	8.3	5.1

227

228 2.4. Experimental design

229 In order to study the influence of non-equilibrium and non-linearity of cesium sorption,
230 four stirred flow-through reactor experiments were conducted, for each soil, under different
231 cesium input concentrations (C_i) and flowrate (Q_i) conditions (**Table 3**). In total, our
232 experimental design combined three levels of cesium concentrations (10^{-3} mol L^{-1}, 10^{-5} mol L^{-1}, and 10^{-8} mol L^{-1}) and two levels of flowrates (10 ml h^{-1} and 35 ml h^{-1}).

234

235 **Table 3.** Experimental conditions of the 4 stirred flow-through reactor experiments conducted
236 for soils S and H. The name of each experimental condition (e.g. "S8-10") indicates the
237 combination of soil name (i.e. S or H), approximate cesium input concentration C_i (i.e.10^{-3},
238 10^{-5} or 10^{-8} mol L^{-1}) and approximate flowrate Q_i (i.e. 10 or 35 mL h^{-1}).

Properties		**Experiments**							
		S3-10	**S5-35**	**S8-10**	**S8-35**	**H3-10**	**H5-35**	**H8-10**	**H8-35**
	Soil	S	S	S	S	H	H	H	H
Q_i	Average flow rate (mL h^{-1})	10.62	33.48	9.66	34.38	9.72	34.02	9.36	31.98
C_i	Cesium concentration (mol L^{-1})	9.97E-04	9.71E-06	6.57E-09	6.92E-09	1.04E-03	9.97E-06	1.21E-08	1.00E-08
T_i	Stage II duration (h)	141	92	262	194	140	71	671	294
	Stage III duration (h)	263	192	938	602	338	195	1967	992
	Stages II+III duration (h)	404	284	1200	796	478	266	2638	1286
m	Soil mass (g)	3.70	3.78	3.78	3.57	2.83	3.12	3.06	3.09
V_r	Reactor water volume (mL)	33.5	33.5	33.5	33.5	33.5	33.5	33.5	33.5

239

2.5. Empirical model of cesium sorption in stirred flow-through reactors

The 5-parameter sorption model EK5 considered here is a generalized version of an empirical linear non-equilibrium sorption EK model (Chaif et al., 2021; Garcia-Sanchez et al., 2014; Nicoulaud-Gouin et al., 2016) that can include sorption nonlinearity (**Figure 3**). Sorbed concentrations are distributed between 'fast' sites (C_{s1}) noted type-1 sites that are instantaneously in equilibrium with the aqueous phase –with an equilibrium constant noted K_{d1} (L kg^{-1})– and 'slow' sites (C_{s2}) noted type-2 sites that are governed by kinetic first order mass transfer –with sorption and desorption rates noted k^+ *(L kg^{-1} s^{-1})* and k^- *(s^{-1})* –. Type-1 and type-2 sites are supposed to have maximum sorption capacities ${C_{s1}}^{max}$ (mol kg^{-1}) and ${C_{s2}}^{max}$ (mol kg^{-1}), as supported by experimental Cesium isotherms (e.g. Cherif et al,. 2017 ; Siroux et al,. 2021), and their sorbed concentrations are modelled by a Langmuir isotherm and a Langmuir kinetic equation (e.g. Selim et al., 1976; Fukui, 1978):

$$C_{s1} = \frac{K_{d1}}{1+\frac{K_{d1}}{C_{s1}^{max}}C_w} C_w \quad (1)$$

$$\frac{dC_{s2}}{dt} = k^+\left(1-\frac{C_{s2}}{C_{s2}^{max}}\right)C_w - k^- C_{s2} \quad (2)$$

The affinity to cesium is quantified by the solid/liquid concentration ratio at equilibrium in the absence of saturation ($C_{s1} \ll {C_{s1}}^{max}$, $C_{s2} \ll {C_{s2}}^{max}$). For type-1 sites, it corresponds by definition to the equilibrium constant K_{d1}. For type-2 sites, the solid/liquid concentration ratio tends to the equilibrium constant K_{d2} (L kg^{-1}) defined by:

$$K_{d2} = \frac{k^+}{k^-}$$

which thus defines their affinity to cesium.

This general formulation contains 3 model variants, noted K_d, EK3 and EK5, relying on embedded hypotheses about type-1 and type-2 sorption sites (**Table 4**). The equations (1) and (2) of EK5 model encompass the 3-parameter linear EK model (noted EK3), which corresponds to the particular case of infinite sorption capacities C_{s1}^{max} and C_{s2}^{max}. They also encompass the classical 1-parameter K_d approach, which only considers type-1 sites, and corresponds to the particular case where $k^+ = 0$ and $k^- = 0$ and infinite C_{s1}^{max}.

In a stirred flow-through reactor with solid-liquid exchanges governed by the EK5 model, conservation equations for the exchangeable stock S_{ex} (mol) in solution and on type-1 sites, and for the fixed stock S_{fix} (mol) on type-2 sites, are then given by:

$$\frac{dS_{ex}}{dt} = -k^+ m\left(1 - \frac{C_{s2}}{C_{s2}^{max}}\right) C_w + k^- S_{fix} + Q_i[C_i\delta(t) - C_w] \quad (3)$$

$$\frac{dS_{fix}}{dt} = k^+ m\left(1 - \frac{C_{s2}}{C_{s2}^{max}}\right) C_w - k^- S_{fix} \quad (4)$$

where C_w (mol L^{-1}) is the dissolved cesium concentration, Q_i (L s^{-1}) is the flowrate, $\delta(t)$ is equal to 1 during contamination stage II and 0 otherwise, m is the soil mass. Exchangeable (S_{ex}) and fixed (S_{fix}) stocks are related to sorbed concentrations as follows:

$$S_{ex} = V_r C_w + mC_{s1} \quad (5)$$

$$S_{fix} = mC_{s2} \quad (6)$$

The system of equations (3)-(6) was implemented within the R environment (R Core Team, 2021) and was solved with the initial conditions $C_w(0)=0$, $C_{s1}(0)=0$ and $C_{s2}(0)=0$. In the case of solid-liquid exchanges governed by the K_d approach, equations (3)-(6) result in the following analytical solution for the breakthrough curve $C_w(t)$:

$$C_w(t) = C_i\left(1 - e^{-\frac{Q}{RV_r}t}\right) \quad if \quad t \le T_i \quad (7)$$

281 $$C_w(t) = C_w(T_i)e^{-\frac{Q}{RV_r}(t-T_i)} \quad if \quad t > T_i \tag{8}$$

282 where the retardation factor R corresponds in this case to:

283 $$R = 1 + \frac{m}{V_r}K_d \tag{9}$$

284 In the general case, the system (3)-(6) was solved numerically with variable time steps by
285 an implicit finite-differences scheme. The implicit Radau IIA scheme, available in the R
286 package "deSolve" (Soetaert et al., 2010), was chosen for its stability, 5th order accuracy and
287 tolerance to stiff equations.

288 As a consequence of the mass-balance equations (3)-(4) above, half-times of sorption and
289 desorption reactions T^+ (s) and T^- (s) in a stirred flow-through reactor can be defined as
290 follows:

291 $$T^+ = \frac{\log(2)V_r}{mk^+} \tag{10}$$

292 $$T^- = \frac{\log(2)}{k^-} \tag{11}$$

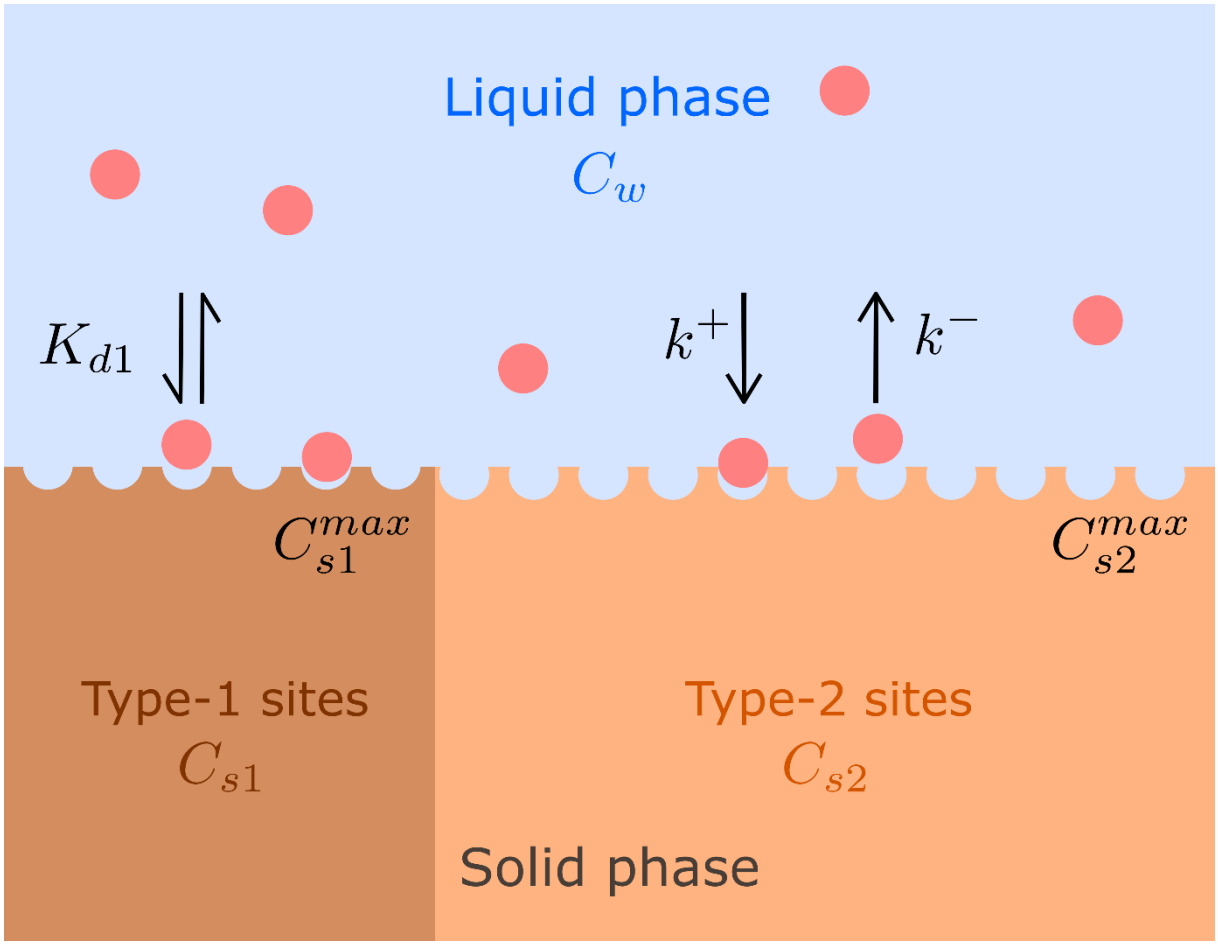

293
294

295 **Figure 3.** Compartment representation of the 5-parameter Equilibrium-Kinetic model EK5
296 applied to Cs sorption in this study. The model considers two types of solid sites for sorption.
297 Type-1 sites are governed by equilibrium parameter K_{d1} (L kg^{-1}). Type-2 sites are controlled
298 sorption by first-order sorption and desorption constants k^+ (L kg^{-1} s^{-1}) and k^- (s^{-1}). $C_{s1}{}^{max}$ (mol
299 kg^{-1}) and $C_{s2}{}^{max}$ (mol kg^{-1}) denote the sorption capacities of type-1 and type-2 sites.
300 Contaminant concentrations are denoted C_w (mol L^{-1}) in water, and C_{s1}, C_{s2} (mol kg^{-1}) in the
301 solid phase.

302

Table 4. Parameters and hypotheses of the model variants K_d, EK3 and EK5 tested in this study to model Cesium sorption. These 3 special formulations derive from equations (1) and (2). EK5 corresponds to the full model, whereas K_d and EK3 introduce additional hypotheses about sorption (the absence of nonlinearity and non-equilibrium) that numerically correspond to particular fixed values for the sorption parameters k^+, k^-, $C_{s1}{}^{max}$ and $C_{s2}{}^{max}$.

Model variant	Sorption hypotheses	Free parameters	Fixed parameters
K_d	Linear equilibrium (type-1)	K_{d1}	$k^+=0, k^-=0$ $C_{s1}{}^{max}=\infty$
EK3	Linear equilibrium (type-1)+ Linear non-equilibrium (type-2)	K_{d1}, k^+, k^-	$C_{s1}{}^{max}=C_{s2}{}^{max}=\infty$
EK5	Nonlinear equilibrium (type-1) + Nonlinear non-equilibrium (type-2)	$K_{d1}, k^+, k^-, C_{s1}{}^{max}$ $C_{s2}{}^{max}$	-

2.6. Estimation of sorbed cesium stocks

Sorbed cesium stocks Q_s (mol) were estimated at the end of contamination and decontamination stages II and III of each experiment in order to quantify cesium retention for the different experimental conditions. Calculations were derived from a mass-balance approach, and were based on the surface area separating breakthrough curves of cesium $C(t)$ and of an inert tracer $C^{tr}(t)$ submitted to the same experimental conditions (Limousin et al., 2007; Martin-Garin et al., 2003). At any time t during the experiment, the sorbed cesium stock Q_s (mol) is governed by:

$$Q_s(t) = V_r\left(C^{tr}(t) - C(t)\right) + \int_0^t Q\left(C^{tr}(\tau) - C(\tau)\right) d\tau \qquad (12)$$

This formula was solved by numerical integration with the experimental concentrations $C_w(t)$ for cesium (eq. 3) and the analytical solution $C^{tr}(t)$ for the inert tracer, which is given by:

$$C^{tr}(t) = C_i\left(1 - e^{-\frac{Q}{V_r}t}\right) \quad if \quad t \le T_i \qquad (13)$$

322 $$C^{tr}(t) = C^{tr}(T_i)e^{-\frac{Q}{V_r}(t-T_i)} \quad if \quad t > T_i \qquad (14)$$

323 with the convention that $t=0$ at the beginning of contamination stage II.

324 In equation (12), C_w/C_i values that were superior to 1 during stage II (and have no physical
325 significance) were considered to be equal to 1 in order to avoid the underestimation of sorbed
326 stocks.

327

328 ## 2.7. Model calibration and local identifiability

329 Sorption parameters of models K_d, EK3 and EK5 were estimated by the least squares method,
330 similarly to *in situ* calibrations detailed by Chaif et al. (2021). Briefly, the normalized
331 dissolved concentration $y_j=C_w/C_i$ was chosen as the observed variable in order to balance the
332 weight of each experiment. To ensure the convergence to an absolute optimum, the sum of
333 squares was minimized numerically from ten starting points by using the R routine "*optim*" (R
334 Core Team, 2021). These starting points had the least sum of squares among a large set of
335 candidate points evaluated in the parameters space (1000 for K_d model, 12^3 for EK3 model,
336 and 12^5 for EK5 model). The likelihood ratio statistic (LR) was used to test hypotheses about
337 sorption models (e.g. K_d vs EK3) (Huet et al., 2004). Confidence regions of estimated Cs
338 sorption parameters $\hat{\vartheta}$ for K_d, EK3 and EK5 models were approximated, at the level 100*(1 -
339 α)%, by the points in the parameters space satisfying the Beale's condition (Beale, 1960;
340 Seber and Wild, 1989). For each individual parameter $\hat{\vartheta}_i$, conservative confidence intervals
341 were then defined as the upper/lower bounds for ϑ_i in this region.

342 Identifiability, i.e. the unicity of the solution to the inverse problem, was diagnosed by the
343 conditioning number κ of the sensitivity matrix (Belsley et al., 1980; Brun et al., 2001;
344 Stewart, 1987), as fully described for reactor experiments by Nicoulaud-Gouin et al. (2016).

345 Conditioning numbers κ above 5 (resp. 10) were interpreted as moderately (resp. strongly)

346 non identifiable parameters (Belsley et al., 1980).

347

3. RESULTS

3.1 Experimental breakthrough curves

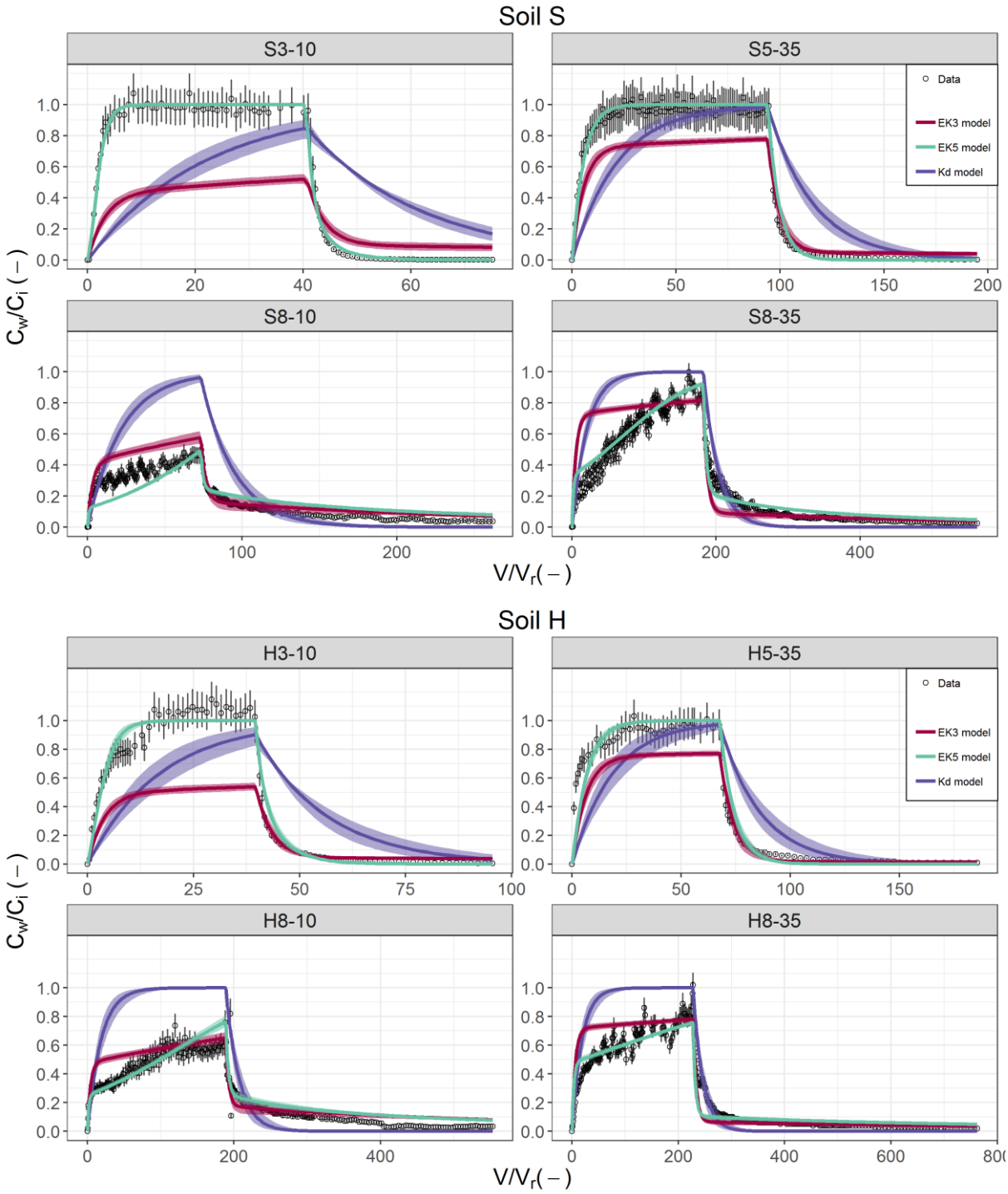

Figure 4. Curves of normalized concentrations C_w/C_i at reactor outlets as a function of normalized volume passing through the reactor V/V_r (breakthrough curves, also noted BTC).

354 Dots correspond to observations and color lines correspond to least squares fits with the K_d
355 (purple), EK3 (red) and EK5 (green) models. Vertical bars correspond to the confidence
356 intervals of the observations. Purple, red, and green shaded bands correspond to the 95%
357 parametric uncertainty of fitted curves.

358

359 For both soils, our observations evidenced influences of flowrate and input concentrations
360 on cesium sorption and thus support the non-equilibrium and nonlinear hypotheses (**Figure**
361 **4**).

362 Cesium outlet concentrations C_w/C_i during contamination stage II systematically increased
363 with flowrate. For instance, the input concentration was completely transmitted to the outlet
364 (C_w/C_i =1) after a cumulated flowed volume V of around 200 reactor volumes (V_r) at 35 mL
365 h^{-1} (experiments S8-35 and H8-35), whereas the breakthrough was still incomplete at 10 mL
366 h^{-1} at the end of contamination stage II (C_w/C_i below 0.6 for experiments S8-10 and H8-10).
367 This trend indicates a smaller sorption when contact time with cesium decreases. These
368 observations prove the influence of non-equilibrium in cesium sorption processes for the
369 studied soils.

370 Cesium outlet concentrations C_w/C_i during contamination stage II systematically increased
371 when input concentration increased. For high input concentrations (10^{-3} mol L^{-1}), the
372 equilibrium state, corresponding to C_w/C_i = 1, was reached after the injection of 10-25 reactor
373 volumes V_r (S3-10 and H3-10) whereas for low concentrations (10^{-8} mol L^{-1}) it was not
374 achieved even after 80-200 V_r (C_w/C_i = 0.46 and C_w/C_i = 0.63 for S8-10 and H8-10
375 respectively). This trend indicates less soil capacity to fix cesium at higher dissolved
376 concentrations. These observations prove the influence of nonlinearity on cesium sorption
377 processes for the studied soils.

Cesium sorption was also affected by the nature of the soils. While similar input conditions provided similar BTC shapes for both soils, some differences in the equilibrium time were observed between the two soils. Convergence to equilibrium state was always faster for soil S than for H. For instance, outlet concentration was stabilized after the injection of 30 V_r for S5-35 compared to 50 V_r for H5-35.

3.2. Sorbed concentrations and restitution

Estimated sorbed stocks during contamination and decontamination stages II and III also revealed influences of flowrate and input concentrations on the reversibility of cesium sorption (**Table 5**).

Cesium desorption during decontamination stage III (termed here restitution) increased with injection concentration and indicated more reversible processes. For high injection concentration experiments (above 10^{-5} mol L^{-1}), restitution was always over 65% for both soils. At low injection concentrations (10^{-8} mol L^{-1}), restitution did not exceed 50% and was around 34% (S8-10) at low flowrate and reached around 47% at high flowrate (S8-35).

Cesium restitution also increased with flowrate. For instance, restitution was around 35% for low flowrate experiments (S8-10 and H8-10) and reached around 45% with higher flowrate (S8-35 and H8-35).

Table 5. Experimental and EK5 simulated stocks of Cs at the end of contamination and decontamination stages II and III as defined in equation (12). Restitution is defined at the ratio of the desorbed and sorbed stocks of Cs.

Conditions	Calculation	Stock at end of stage II (mol)	Stock at end of stage III (mol)	Restitution (%)
S3-10	**Experiment**	6.38E-05	2.51E-05	61
	EK5	7.13E-05	7.46E-08	100
S5-35	**Experiment**	2.17E-06	7.70E-07	64
	EK5	1.77E-06	1.43E-08	99
S8-10	**Experiment**	1.02E-08	6.74E-09	34
	EK5	1.16E-08	6.66E-09	43
S8-35	**Experiment**	1.62E-08	8.54E-09	47
	EK5	1.47E-08	5.33E-09	64
H3-10	**Experiment**	1.32E-04	4.28E-05	68
	EK5	1.32E-04	5.76E-08	100
H5-35	**Experiment**	2.15E-06	4.49E-08	98
	EK5	2.24E-06	4.82E-08	98
H8-10	**Experiment**	3.95E-08	2.63E-08	33
	EK5	3.88E-08	1.79E-08	54
H8-35	**Experiment**	2.92E-08	1.70E-08	42
	EK5	2.93E-08	1.69E-08	42

3.3. Cesium sorption modelling

For both soils, EK5 model described significantly better the observed non-equilibrium and nonlinear effects than EK3 and K_d models.

Qualitatively, the model EK5, with 5 degrees of freedom, better fitted the breakthrough curves than EK3 and K_d models (3 and 1 degrees of freedom) (**Figure 4**). With a constant retardation factor R (eq. 9) for all conditions, the K_d model underestimated C_w/C_i at high input concentration values and overestimated them at low concentration values (C_w/C_i=1 at the end of stage II of all experiments). With kinetic rates of sorption and desorption allowing asymmetry in the curves between stages II and III, EK3 model better fitted C_w/C_i during stage

410 III whereas it was still unrealistic during stage II (S5-35, H3-10, and H5-35 for example).
411 With sorption capacities potentially limiting the sorption on type-1 and type-2 sites, EK5
412 model better described the strong inflexions of C_w/C_i during stage II for all experiments with
413 two exceptions being S8-10 where sorption was slightly overestimated at the start of stage II,
414 and H8-10 where sorption was underestimated at the end of stage II.

415 Sorbed stocks predicted by the EK5 model showed two distinct behaviors depending on
416 the input concentrations (**Table 5**). At high concentrations, sorption was completely reversible
417 with restitution rates superior to 98% for both soils. At low concentrations, sorption was
418 irreversible and restitution never exceeded 64%. These results suggest that EK5 model can
419 reproduce both reversible and irreversible behaviors depending on the experimental
420 conditions using the same set of parameters.

421 Quantitatively, the better performance of EK5 model vs EK3 and K_d was confirmed
422 statistically for both soils by the likelihood ratio tests (**Table 6**). Even though the inclusion of
423 non-equilibrium sorption significantly improved the fit (EK3 vs K_d), the addition of nonlinear
424 sorption made it even better, as indicated by p-values always under 10^{-16} for the likelihood
425 ratio test of model EK3 vs model EK5. These results prove that the formulation of sorption
426 nonlinearity and non-equilibrium proposed by model EK5, although still very simple, brings a
427 significant improvement to EK3 and K_d alternatives and suggest its applicability to various
428 soils.

429

Table 6. Statistics summary of the fits of sorption models (K_d, EK3 and EK5). For each soil, sorption models were fitted simultaneously on the 4 stirred flow-through reactor experiments. Sum of squares S denotes the sum of squared errors between model predictions and observations. The p-value of the Likelihood ratio (LR) statistic was derived from its approximate chi-squared distribution, as detailed in Chaif et al. (2021).

Quantity		Soil S	Soil H
Sum of squares S	K_d model	65.4	51.7
	EK3 model	29.6	17.4
	EK5 model	3.50	4.43
K_d vs EK3	LR	665	786
	p-value	<1e-16	<1e-16
K_d vs EK5	LR	2455	1771
	p-value	<1e-16	<1e-16
EK3 vs EK5	LR	1790	985
	p-value	<1e-16	<1e-16

3.4 Fitted parameters

For both soils, fitted EK5 parameters suggested very contrasted conditions of cesium sorption between equilibrium and non-equilibrium sites in terms of characteristic sorption times, affinity and sorption capacity (**Table 7**).

The type-1 equilibrium sites had a very high sorption capacity, as indicated by C_{s1}^{max} values comparable to soil CEC (**Table 1**), but had a non-specific affinity to cesium, as indicated by low K_{d1} values (40 - 60 L kg^{-1} depending on the soil).

443 The type-2 non-equilibrium sites had a fast sorption rate k^+ and a slow desorption rate k^-.
444 Sorption half-times T^+ of less than one hour for both soils (0.2 and 0.3 hours on average for
445 soils S and H respectively) were shorter than mean residence time of solution in the reactors
446 (0.96 to 3.35 hours depending on the flowrate) and indicated a fast cesium sorption.
447 Desorption half-times T^- were much longer (3 and 9 days on average for soils S and H
448 respectively) and suggested a pseudo-irreversible cesium sorption.

449 The type-2 non-equilibrium sites had a very strong affinity to cesium but with a very
450 limited sorption capacity. They had a specific affinity to cesium, as indicated by large values
451 of their theoretical equilibrium ratio $K_{d2} = k^+/k^-$ (3489 to 6171 L kg^{-1} for soils S and H
452 respectively). Their sorption capacity C_{s2}^{max} was very small (0.04% and 0.02% of the CEC of
453 soils S and H respectively) and indicated a very limited number of type-2 sites.

454 Soil H had a higher cesium sorption capacity than Soil S. Distribution coefficient of both
455 equilibrium and kinetic sites K_{d1} and K_{d2} were respectively 51% and 77% higher in soil H
456 than in S. Similarly, equilibrium and kinetics sites saturations C_{s1}^{max} and C_{s2}^{max} were 456%
457 and 260% higher in H than S. These values are in line with the contrasted physiochemical and
458 mineralogical properties of the two soils, notably the higher CEC and clay and organic matter
459 content of soil H compared to S (**Table 1**).

460

461 **Table 7.** Fitted parameter values of the EK5 model. Values correspond to ordinary least-
462 squares estimations, and intervals correspond to conservative 95% confidence intervals.

Parameter	Unit	Soil S	Soil H
K_{d1}	L kg^{-1}	40 [34 ; 46]	60 [49 ; 74]
k^+	L kg^{-1} s^{-1}	4.71E-03 [4.27E-03 ; 5.24E-03]	2.45E-03 [2.20E-03 ; 2.73E-03]
k^-	s^{-1}	1.35E-06 [1.15E-06 ; 1.59E-06]	3.98E-07 [3.07E-07 ; 5.01E-07]
C_{s1}^{max}	mol kg^{-1}	1.38E-02 [1.01E-02 ; 1.92E-02]	7.67E-02 [4.94E-02 ; 1.39E-01]
C_{s2}^{max}	mol kg^{-1}	4.83E-06 [4.49E-06 ; 5.21E-06]	1.74E-05 [1.55E-05 ; 2.01E-05]

463

4. DISCUSSION

4.1. Experimental design

Our experimental design (combining 3 concentration levels and 2 flowrate levels in 4 experiments) allowed to identify uniquely and accurately the EK5 parameters for both soils. The conditioning numbers κ (2.291 and 2.505) well below 5 indicated *a posteriori* that our experimental design constrained the fitted equations (3)-(4) to a unique set of parameter values (**Table 8**). The good identifiability of EK5 parameters was also confirmed numerically by the narrow confidence intervals of parameters, whose half-width did not exceed 16% for Soil S and 26% for Soil H (**Table 7**).

These numerical results suggest the adoption of our 4 reactor design for future CSTR experiments aiming at identifying EK5 parameters for other soils/radionuclides. They are complementary to more formal analyses recommending at least 2 experiments for the identification of the EK3 model (Nicoulaud-Gouin et al., 2016).

Considering that EK5 model well fitted the BTC curves, the EK5 parameters obtained in this study can be seen as simple but accurate indicators of sorption processes, and, as such, deserve further discussion about their physical interpretation.

Table 8. Local identifiability of EK5 parameters for soils S and H, as diagnosed from the conditioning number κ of the sensitivity matrix (Brun et al., 2001). The applied formulae are fully detailed in Nicoulaud-Gouin et al. (2016).

	Notation	Soil S					Soil H				
Eigenvalues	λ_i	2.079	1.155	0.862	0.508	0.396	2.025	1.398	0.724	0.530	0.323
Conditioning number	κ	2.291					2.505				

4.2. Physical nature of type-1 and type-2 sites

Since cesium sorption in soils is primarily governed by clay minerals (Bostick et al., 2002; Chorover et al., 2003; Missana et al., 2014a; Savoye et al., 2012; Shenber and Eriksson, 1993; Wendling et al., 2005), it seems plausible that the equilibrium and kinetic sites postulated by the EK5 model are an empirical typology of the various clay sorption sites.

The non-linearity of Cs sorption is mainly due to the heterogeneity of the surface adsorption sites (Bradbury and Baeyens, 2000; Cornell, 1993; Eliason, 1966; Missana et al., 2004; Poinssot et al., 1999; Staunton and Roubaud, 1997; Wahlberg and Fishman, 1962) which, as reviewed in introduction, broadly includes interlayer sites with low density strong affinity to cesium but and planar sites with higher densities but lower affinity cesium. These observations have been summarized quantitatively with a simplified two-site thermodynamic model of Cs sorption on clay noted 1-pK DL/IE (Cherif et al., 2017). The first sites are governed by an ion exchange (IE) model which simulates the adsorption of Cs on negatively charged sites of planar surface of clay minerals, including outer-basal and interlayers sites ($\equiv X^-$). The second sites are governed by a surface complexation (SC) model used to describe the adsorption of cations on a single FES site ($\equiv S0^{-0.5}$) (Cherif et al., 2017 and references therein). A database of these sites densities is available for illite, montmorillonite and kaolinite minerals. Therefore, for a given soil, knowing its mineralogical composition allows the estimation of IE and surface complexation sites densities (**Table 9**).

The densities of type-1 equilibrium sites (given by C_{s1}^{max}) and type-2 kinetic sites (given by C_{s2}^{max}) of EK5 model seem to correspond to those of IE and SC sites of clay minerals of both soils respectively (**Table 9**). On one hand, IE sites densities were almost identical to C_{s1}^{max} for soil S (relative error of 5%) and around two times higher for soil H. On the other

hand, the offset between C_{s2}^{max} and surface complexation sites densities was of a similar magnitude for both soils (relative error of 80% and 52% for S and H respectively). These differences can be explained by : (1) the presence of other sites, mainly organic matter, that can contribute to cesium sorption (Nakamaru et al., 2007; Rigol et al., 2002; Valcke and Cremers, 1994); (2) The uncertainty related to the estimation of proportions of the clay minerals (illite, montmorillonite and kaolinite available in the soils). In fact, the XRD method used to estimate these proportions is semi-quantitative and only provides a gross estimation of these proportions (**Table 1**).

With parameters values of C_{s1}^{max} and C_{s2}^{max} fixed to Exchange and surface complexation sites densities of the studied soils (**Table 9**), the model EK5 yielded satisfactory predictions of BTC (**Figure 5**). The model EK5 satisfactorily reproduced all the experimental breakthrough curves except for experiments S8-10 and S8-35, where predicted concentrations C_w/C_i increased towards unity earlier than observed. This is mainly due to the surface complexation sites density being slightly lower than C_{s2}^{max} which lead to a premature saturation of kinetic sites at the end of stage II of experiment S8-10. The exchange and surface complexation sites densities seem to provide a good first indicator of the sorption capacities of equilibrium and kinetic sites. However, the uncertainties associated with the proportions of minerals and their IE and SC densities may explain the imprecise estimation of the C_{s1}^{max} and C_{s2}^{max} parameters.

527 **Table 9.** Exchange and surface complexation sites densities derived from the mineralogical
528 properties of the studied soils and the properties of illite, montmorillonite and kaolinite
529 compiled by Cherif et al. (2017). Cation exchange capacity (CEC) (from **Table 1**) and fitted
530 sorption capacities C_{s1}^{max} and C_{s2}^{max} (from **Table 7**) are recalled here to support the
531 comparisons given in the text.

	Soil S			Soil H		
	Min	**Mean**	**Max**	**Min**	**Mean**	**Max**
Ion Exchange "IE" sites density (mol kg^{-1})	1.19E-02	1.31E-02	1.43E-02	1.53E-01	1.80E-01	2.07E-01
CEC (mol kg^{-1})		1.11E-02			7.64E-02	
C_{s1}^{max} (mol kg^{-1})	1.01E-02	1.38E-02	1.92E-02	4.94E-02	7.67E-02	1.39E-01
Surface complexation sites density (mol kg^{-1})	6.59E-07	9.77E-07	1.30E-06	2.63E-05	3.66E-05	4.70E-05
C_{s2}^{max} (mol kg^{-1})	4.49E-06	4.83E-06	5.21E-06	1.55E-05	1.74E-05	2.01E-05

532

533

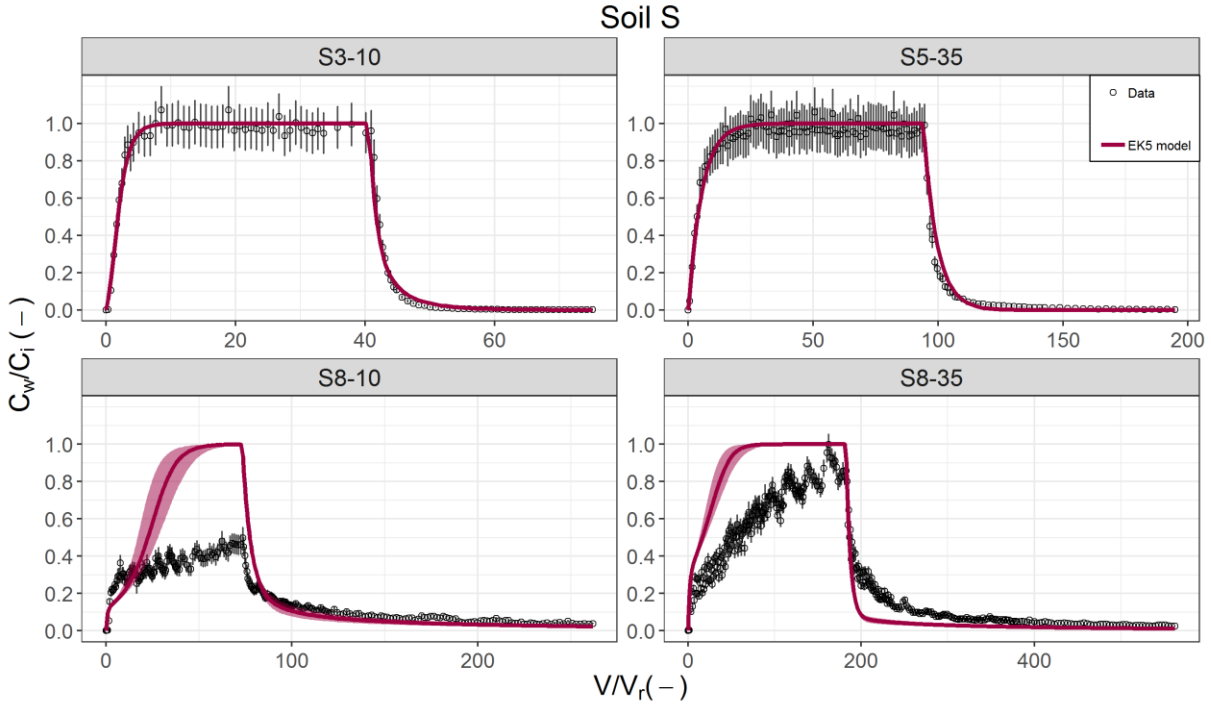

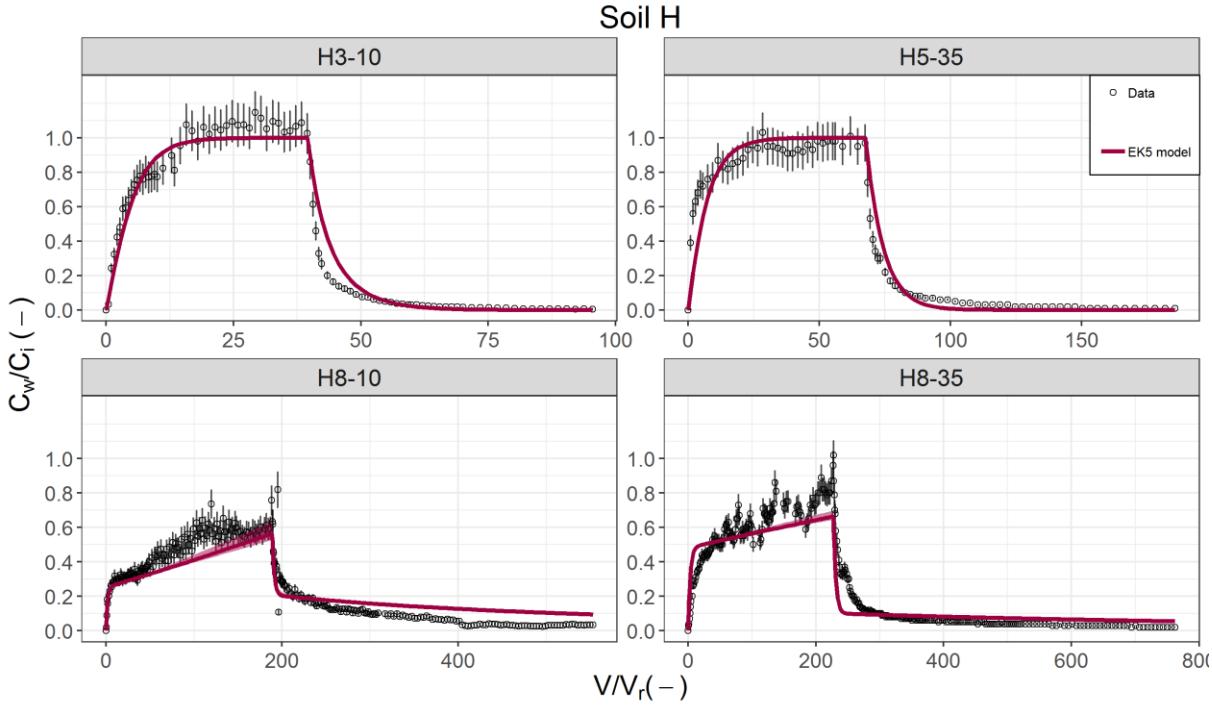

Figure 5. Cs breakthrough curves simulated by the EK5 model with C_{s1}^{max} (resp. C_{s2}^{max}) equal to the ion exchange (resp. surface complexation) sites densities (**Table 9**). Other parameters (K_{d1}, k^+, and k^-) were at fitted values (**Table 7**).

4.3. Cesium sorption and reversibility on equilibrium and kinetic sites

The EK5 hypothesis better reproduced the experimental results by considering that sorption sites act differently at low, intermediate and high concentrations of cesium (**Figure 6**).

At low input concentrations (10^{-8} mol L^{-1}), simulated Cs sorbed on type-2 sites without saturation of sorption capacity at the end of contamination stage II (e.g. 60% for S8-10 and 80% for S8-35). Simulated Cs sorption on type-1 sites was virtually inexistent (with saturation index almost at 0%) due to their much lower affinity to Cs. As a consequence, simulated Cs desorption during decontamination stage III resulted only from type-2 sites.

At high input concentrations (10^{-3} mol L^{-1}), simulated Cs also initially sorbed on type-2 sites. However, type-2 sites rapidly reached saturation (less than one hour), and simulated Cs continued to sorb on type-1 sites without saturation at the end of contamination stage II (e.g. around 75% for S3-10 and 45% H3-10). Considering that type-1 sites held almost all the sorbed inventory, simulated Cs desorption during decontamination stage III resulted only from type-1 sites.

At intermediate input concentrations (10^{-5} mol L^{-1}), simulated Cs initially sorbed on type-2 sites (at short times) and on type-1 sites during contamination stage II. During decontamination stage III, type-1 and type-2 sites both contributed to desorption in the opposite order. Indeed, simulated Cs initially desorbed exclusively from low affinity type-1 sites. After type-1 sites were rapidly decontaminated (less than 6 hours), simulated Cs continued to desorb from high affinity type-2 sites and this process was much slower.

This behavior of the EK5 model is consistent with studies evidencing specific and non-specific cesium sorption in soils. In fact, several studies conducted on clay minerals (illite,

563 montmorillonite and kaolinite) have shown that cesium sorption takes place on two distinct
564 sites with different affinities (Benedicto et al., 2014; Brouwer et al., 1983; Missana et al.,
565 2014b; Poinssot et al., 1999; Staunton and Roubaud, 1997). The sorption isotherms obtained
566 in these studies showed that cesium sorption depended on the cesium concentration in the
567 solution. At low concentrations, cesium sorption was the highest and decreased when cesium
568 concentrations increased.

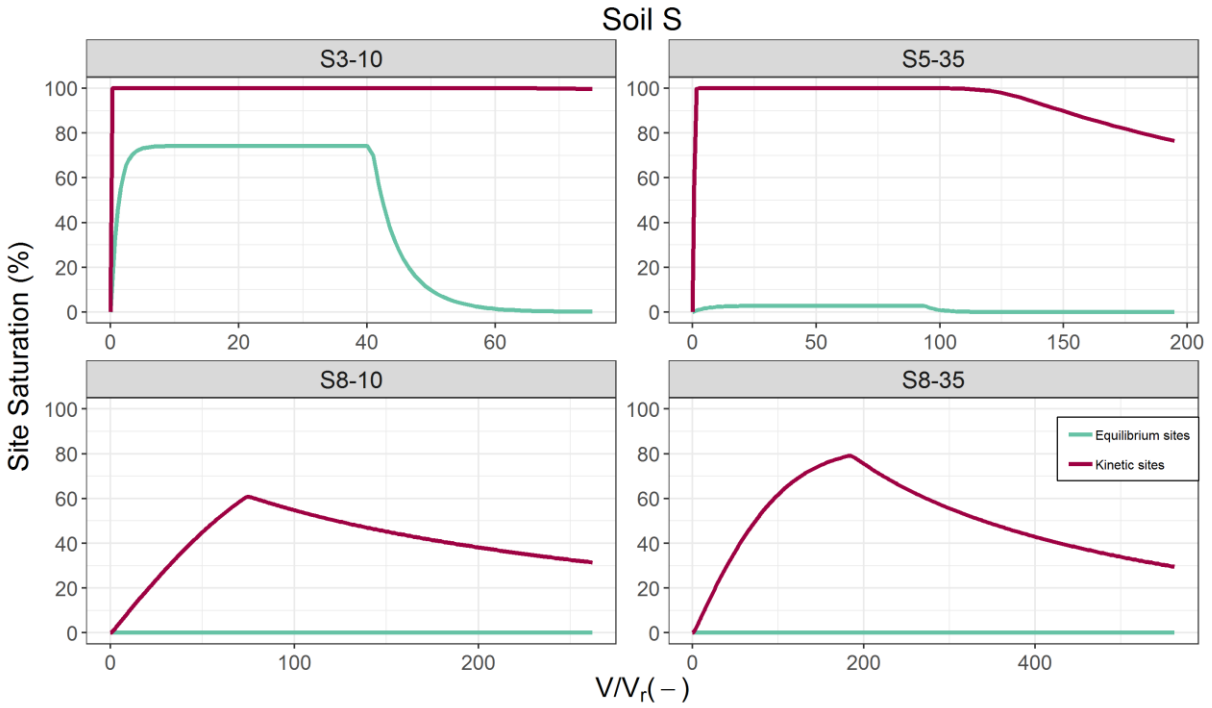

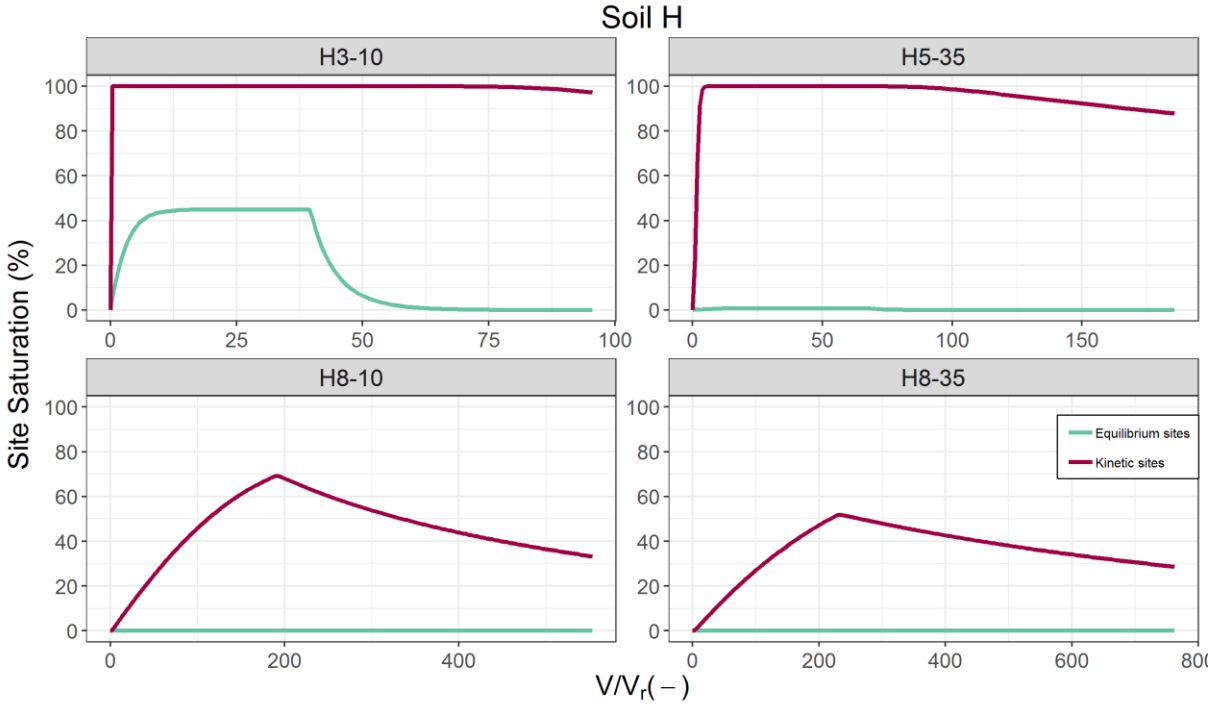

Figure 5. Percentage of occupied sites for type-1 equilibrium (green) and type-2 kinetic (red) sites, as simulated by the EK5 model with fitted parameters (**Table 7**). Cumulated flowed volume at the reactor outlet V is normalized by the volume V_r of the reactor chamber.

4.4. Domains of sorption nonlinearity and non-equilibrium

Rewriting the equations of reactive transport (3)-(4) can reveal when nonlinear and non-equilibrium effects are significant (and the full EK5 model is required) and when linearity or equilibrium hypotheses are appropriate (and K_d or EK3 models can be used).

In the case of the EK3 model, the reactive transport equations (3) and (4) have been rewritten in a simplified form by introducing the following transformations (Nicoulaud-Gouin et al., 2016):

$$C_w^* = \frac{C_w}{C_i}\ ; \quad C_{s2}^* = \frac{m}{V_r}\frac{C_{s2}}{C_i}; \quad t^* = \frac{Q_i t}{V_r}; \quad D_{a1} = \frac{mk^+}{Q_i}; \quad D_{a2} = \frac{V_r k^-}{Q_i}; \; K_{d1}^* = \frac{m}{V_r}K_{d1}$$

where C_w* and C_{s2}* are dimensionless concentrations in solution and on type-2 sites, t* is dimensionless time, D_{a1} and D_{a2} are ratios of sorption and desorption times to water residence time, also known as Damköhler numbers (Bahr and Rubin, 1987). In the case of the full EK5 model, reactor equations (3) and (4) here write:

$$\frac{dC_w^*}{dt^*} = -\frac{1+D_{a1}(1-\tau_2)}{R(C_w^*)}C_w^* + \frac{D_{a2}}{R(C_w^*)}C_{s2}^* + \frac{\delta}{R(C_w^*)} \tag{15}$$

$$\frac{dC_2^*}{dt^*} = D_{a1}(1-\tau_2)C_w^* - D_{a2}C_2^* \tag{16}$$

$$R(C_w^*) = 1 + \frac{K_{d1}^*}{\left(1+\frac{K_{d1}^*}{C_{s1}^{max*}}C_w^*\right)^2} \tag{17}$$

where R is the retardation factor due to type-1 sites. The dimensionless sorption capacity C_{s1}^{max*} of type-1 sites and the rate of occupied type-2 sites τ_2 are defined by:

$$C_{s1}^{max*} = \frac{m}{V_r}\frac{C_{s1}^{max}}{C_i}; \qquad \tau_2 = \frac{C_{s2}}{C_{s2}^{max}}$$

In equation (15), type-2 sorption of a contaminant is significant if $D_{a1} > 1$, or equivalently if the half-time of the sorption reaction T^+ is shorter than water residence time ($T^+ < T_w$). Similarly, type-2 desorption of a contaminant can occur significantly if $D_{a2} > 1$, or equivalently if the half-time of the desorption reaction T^- is shorter that water residence time ($T^- < T_w$). As a consequence, the condition ($T_w < T^+$ or $T_w < T^-$) corresponds to the non-equilibrium sorption domain, and in particular, the domain $T_w << T^-$ corresponds to pseudo-irreversible sorption (**Figure 7**).

Type-1 sorption is governed by a Langmuir isotherm (eq. 1) and tends to saturate when $K_{d1}C_W/C_{s1}^{max}$ exceeds 1, which corresponds to C_w greater than C_{s1}^{max}/K_{d1}. Quantitatively, type-1 sites are saturated at 50% when C_w is equal to C_{s1}^{max}/K_{d1}, and are saturated at 99% when C_w is approximately 100 C_{s1}^{max}/K_{d1}. Similarly, from equation (2), type-2 sorption tends at equilibrium to a Langmuir isotherm, which saturates when C_w is greater than C_{s2}^{max}/K_{d2}. As a consequence, dissolved cesium concentrations C_w lying in the intervals $[1,100]*C_{s1}^{max}/K_{d1}$ or $[1,100]*C_{s2}^{max}/K_{d2}$ correspond to the domain of nonlinear sorption (**Figure 7**).

This analysis thus shows that the minimal sorption model depends on the residence time of water (T_w) and the dissolved cesium concentration in water (C_w). Three broad sorption domains can be defined and distinguished in the plane (T_w, C_w) (**Figure 7**): the equilibrium domain (where sorption can be described by an isotherm model, including the K_d model at trace concentrations), the linear equilibrium (where the linear kinetic approximation EK3 applies) and the nonlinear non-equilibrium domain (where the full EK5 cannot be simplified). The nonlinear non-equilibrium domain indicates the reactive transport scenarios for which the EK5 model can improve the realism of predictions.

For scenarios of radiocesium release in the environment, the influence of sorption nonlinearity may not be significant on reactive transport and the approximations of models K_d or EK3 may be valid. Indeed, the linear domain corresponds to dissolved concentrations below C_{s2}^{max}/K_{d2}, i.e. approximately below 1.4 10^{-9} and 2.8 10^{-9} mol L^{-1} for the studied soils S and H. In the case of ^{137}Cs (with mass activity 3.22 10^{12} Bq g^{-1}), this would correspond to maximum concentrations of 71 and 146 kBq L^{-1}. However, nonlinear sorption may occur at much lower concentrations C_w in the presence of stable cesium in the soil and more competing cations in the solution (e.g. Fukui, 1978; Saiers and Hornberger, 1996; Flury et al., 2004).

On the contrary, the influence of non-equilibrium sorption on reactive transport may be critical for common hydrological conditions. In a porous medium of characteristic length L (m) and humidity Θ (-), a characteristic water flux density q_i (m^3 s^{-1} m^{-2}) corresponds to a water residence time:

$$T_w = \frac{q_i}{L\,\Theta}$$

Sorption and desorption can generally be considered instantaneous for Damköhler numbers $Da_1=T_w/T^+$ and $Da_2=T_w/T^-$ higher than 100 (e.g. Bahr and Rubin, 1987). For soils S and H, sorption had very short half-lives T^+ (0.2 and 0.3 h) and can be considered much faster than water residence time in a soil column for common hydrological situations. However, desorption has much longer half-lives T^- (3 and 9 days) and may be often comparable to water residence time. As a result, the equilibrium model K_d may be appropriate for very slow water flows as observed in underground or deep geological nuclear waste repositories (Grigaliūnienė et al., 2020; Medved' and Černý, 2019; Yim and Simonson, 2000). But non-equilibrium model EK3 model seems better appropriate for the fast transient contamination

and infiltration conditions occurring in the unsaturated zone (Ardois and Szenknect, 2005; Brusseau et al., 1989; Maraqa et al., 1999; Testoni et al., 2017).

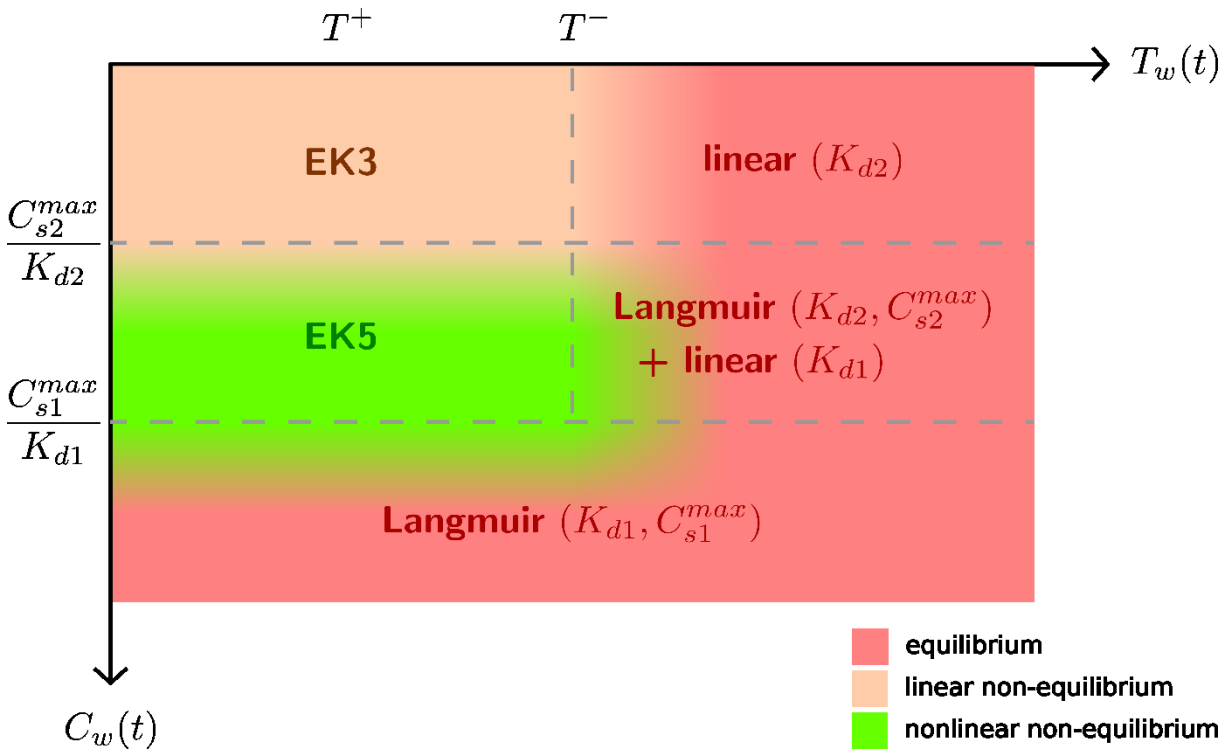

Figure 6. Applicability domains of the models K_d (linear), EK3 and EK5 at a given time t of a reactive transport scenario with mean residence time of water $T_w(t)$ and dissolved cesium concentration $C_w(t)$. This representation is specific to this study, where it was observed that type-2 sorption time T^+ was shorter than desorption time T^-, and that the density of type-2 sorption sites ($C_{s2}{}^{max}$) was much lower than the density of type-1 sites ($C_{s1}{}^{max}$).

5. CONCLUSIONS

This work demonstrated that non-equilibrium and non-linear processes can influence cesium sorption in conditions of reactive transport.

For each studied soil, the 4 stirred flow-through reactor experiments indicated that cesium was less retarded when injected concentrations and/or flow rate increased. The proposed sorption model EK5 reproduced significantly better the experimental observations compared to simpler sorption models (K_d and EK3). It could well reproduce, with a single set of parameters, the four breakthrough curves of cesium observed for both soils in the range 10-35 mL h^{-1} for flow rate and 10^{-8}-10^{-3} mol L^{-1} for injection concentration. For both soils, the fitted EK5 parameters suggested contrasted conditions of cesium sorption between equilibrium and non-equilibrium sites. The equilibrium sites had a sorption capacity comparable to soil CEC, but had a low affinity to cesium (40-60 L kg^{-1}). The non-equilibrium sites had a much shorter sorption half-time (0.2-0.3 hours) compared to half-time of desorption (3-9 days), which allows pseudo-irreversible cesium sorption at high flow rates. The non-equilibrium sites had a strong affinity to cesium (3489-6171 L kg^{-1}) but their sorption capacity only represented 0.02-0.04% of the CEC. The type-1 equilibrium and type-2 kinetic sites postulated by the EK5 model are an empirical representation of soil sorption sites that seems physically sound. They seem to correspond respectively to ion-exchange and surface complexation sites of clay minerals, as suggested by the similarity between their fitted and measured sorption capacities.

From a methodological standpoint, this study also showed that an experimental design combining four flow-through reactor experiments with different conditions of flow rate and injection concentration allows a precise identification of the 5 parameters of the proposed EK5 model. This study also suggested the conditions of Cs reactive transport for which non-equilibrium and nonlinear effects are important and thus variants of the EK5 model may be

668 more realistic than the K_d model. Non-equilibrium sorption effects increase when water
669 residence time decreases and becomes comparable to the half times of sorption and desorption
670 reactions (respectively 1 hour and 6-20 days for the studied soils). Non-linear sorption effects
671 emerge when sorbed Cs concentration is close to sorption capacity limits of type-2 and type-1
672 sites (approximately 1% and 99% of CEC for the studied soils). However, the applicability of
673 proposed EK model calibrated in the laboratory for predicting the reactor transport of Cs *in*
674 *situ* on contaminated soils has not been fully demonstrated yet. The validity and parameter
675 values of the EK5 model derived here from stirred flow-through reactor experiments concern
676 small representative elementary volumes and may no longer apply for complex flows in
677 porous media where other processes of nonlinear and non-equilibrium sorption may emerge.
678 Further experiments on soils with more contrasted physico-chemical properties (e.g. content
679 in clay minerals) and on systems of different levels of complexity (from batch reactors to soil
680 columns) are necessary to generalize the findings of this work.

681

682 **ACKONWLEDGEMENTS**

683 This research was funded by Electricité de France (EDF) and IRSN in the framework of the
684 project GGP-Environnement (v1-300, 2017-2020).

685 **REFERENCES**

686 Antonopoulos-Domis M., Clouvas A., Hiladakis A., Kadi S., 1995. Radiocesium distribution
687 in undisturbed soil: measurements and diffusion-advection model. Health Physics 1995; 69:
688 949-953. https://doi.org/10.1097/00004032-199512000-00009.

689 Ardois C., Szenknect S., 2005. Capability of the Kd model to predict radionuclides behaviour
690 and transport in unsaturated columns under steady flow conditions. Radioprotection 40, S53–
691 S59. https://doi.org/10.1051/radiopro:2005s1-009. Vol 40, 2005.

692 Avery S.V., 1996. Fate of caesium in the environment: distribution between the abiotic and
693 biotic components of aquatic and terrestrial ecosystems. Journal of Environmental
694 Radioactivity 30: 139-171.

695 Bahr J.M., Rubin J., 1987. Direct comparison of kinetic and local equilibrium formulations
696 for solute transport affected by surface reactions. Water Resources Research 23: 438-452.

697 Bar- Tal A., Feigenbaum S., Sparks D.L., Pesek J.D., 1990. Analyses of Adsorption Kinetics
698 Using a Stirred- Flow Chamber: I. Theory and Critical Tests. Soil Science Society of
699 America Journal 54: 1273-1278.

700 Beale E.M.L., 1960. Confidence Regions in Non-Linear Estimation. Journal of the Royal
701 Statistical Society. Series B (Methodological) 22: 41-88.

702 Belsley D.A., Kuh E., Welsch R.E., 1980. Regression diagnostics : identifying influential data
703 and sources of collinearity. John Wiley and sons, Hoboken, New Jersey.
704 http://doi.org/10.1002/0471725153

705 Benedicto A., Missana T., Fernández A.M., 2014. Interlayer collapse affects on cesium
706 adsorption onto illite. Environmental Science & Technology 48: 4909-4915.

707 Bossew P., Kirchner G., 2004. Modelling the vertical distribution of radionuclides in soil. Part
708 1: the convection–dispersion equation revisited. Journal of Environmental Radioactivity 73:
709 127-150.

710 Bostick B.C., Vairavamurthy M.A., Karthikeyan K., Chorover J., 2002. Cesium adsorption on
711 clay minerals: An EXAFS spectroscopic investigation. Environmental Science & Technology
712 36: 2670-2676.

713 Bouzidi A., Souahi F., Hanini S., 2010. Sorption behavior of cesium on Ain Oussera soil
714 under different physicochemical conditions. Journal of Hazardous Materials 184: 640-646.

715 Bradbury M.H., Baeyens B., 2000. A generalised sorption model for the concentration
716 dependent uptake of caesium by argillaceous rocks. Journal of Contaminant Hydrology 42:
717 141-163.

718 Brouwer E., Baeyens B., Maes A., Cremers A., 1983. Cesium and rubidium ion equilibriums
719 in illite clay. The Journal of Physical Chemistry 87: 1213-1219.Brun R., Reichert P., Künsch
720 H.R., 2001. Practical identifiability analysis of large environmental simulation models. Water
721 Resources Research 37: 1015-1030.

722 Brusseau M.L., Jessup R.E., Rao P.S.C., 1989. Modeling the transport of solutes influenced
723 by multiprocess nonequilibrium. Water Resources Research 25: 1971-1988.

724 Cameron D., Klute A., 1977. Convective- dispersive solute transport with a combined
725 equilibrium and kinetic adsorption model. Water Resources Research 13: 183-188.

726 Castrillejo M., Casacuberta N., Breier C.F., Pike S.M., Masqué P., Buesseler K.O., 2016.
727 Reassessment of 90Sr, 137Cs, and 134Cs in the coast off Japan derived from the Fukushima
728 Dai-ichi nuclear accident. Environmental Science & Technology 50: 173-180.

729 Chaif H., Coppin F., Bahi A., Garcia-Sanchez L., 2021. Influence of non-equilibrium sorption
730 on the vertical migration of 137Cs in forest mineral soils of Fukushima Prefecture. Journal of
731 Environmental Radioactivity 232: 106567.

732 Chen G.-N., Li Y.-C., Zuo X.-R., Ke H., Chen Y.-M., 2020. Comparison of Adsorption
733 Behaviors of Kaolin from Column and Batch Tests: Concept of Dual Porosity. Journal of
734 Environmental Engineering 146: 04020102.

735 Cherif M.A., 2017. Dynamic modeling of the (bio)availability of radionuclides in soils: a
736 comparative model-experiment approach applied to the transfer of Cs (I) in the rhizosphere
737 (in french). PhD thesis, Aix-Marseille Université, 2017.
738 http://www.theses.fr/2017AIXM0547.

739 Cherif M.A., Martin-Garin A., Gérard F., Bildstein O., 2017. A robust and parsimonious
740 model for caesium sorption on clay minerals and natural clay materials. Applied
741 Geochemistry 87: 22-37.

742 Chorover J., Choi S., Amistadi M.K., Karthikeyan K., Crosson G., Mueller K.T., 2003.
743 Linking cesium and strontium uptake to kaolinite weathering in simulated tank waste
744 leachate. Environmental Science & Technology 37: 2200-2208.

745 Comans R.N.J., Hockley D.E., 1992. Kinetics of cesium sorption on illite. Geochimica et
746 Cosmochimica Acta 56: 1157-1164.

747 Cornell R.M., 1993. Adsorption of cesium on minerals: A review. Journal of Radioanalytical
748 and Nuclear Chemistry 171: 483-500.

749 Durrant C.B., Begg J.D., Kersting A.B., Zavarin M., 2018. Cesium sorption reversibility and
750 kinetics on illite, montmorillonite, and kaolinite. Science of The Total Environment 610-611:
751 511-520.

752 Eberl D.D., 1980. Alkali cation selectivity and fixation by clay minerals. Clays and clay
753 minerals 28: 161-172.

754 Eliason J., 1966. Montmorillonite exchange equilibria with strontium-sodium-cesium.
755 American Mineralogist: Journal of Earth and Planetary Materials 51: 324-335.

756 Fesch C., Simon W., Haderlein S.B., Reichert P., Schwarzenbach R.P., 1998. Nonlinear
757 sorption and nonequilibrium solute transport in aggregated porous media: Experiments,
758 process identification and modeling. Journal of Contaminant Hydrology 31: 373-407.

759 Fiengo Perez F., Sweeck L., Bauwens W., Van Hees M., Elskens M., 2015. Adsorption and
760 desorption kinetics of 60Co and 137Cs in freshwater rivers. Journal of Environmental
761 Radioactivity 149:81-89. https://doi.org/10.1016/j.jenvrad.2015.07.010

762 Flury M., Czigány S., Chen G., Harsh J.B., 2004. Cesium migration in saturated silica sand
763 and Hanford sediments as impacted by ionic strength. Journal of Contaminant Hydrology 71:
764 111-126.

765 Francis C., Brinkley F., 1976. Preferential adsorption of 137Cs to micaceous minerals in
766 contaminated freshwater sediment. Nature 260: 511-513.

767 Fukui M., 1978. Evaluation of a Combined Sorption Model for Describing Cesium Transport
768 in a Soil. Health Physics 35: 552-562.

769 Fuller A.J., Shaw S., Ward M.B., Haigh S.J., Mosselmans J.F.W., Peacock C.L., Stackhouse
770 S., Dent A.J., Trivedi D., Burke I.T., 2015. Caesium incorporation and retention in illite
771 interlayers. Applied Clay Science 108: 128-134.

772 Garcia-Sanchez L., Loffredo N., Mounier S., Martin-Garin A., Coppin F., 2014. Kinetics of
773 selenate sorption in soil as influenced by biotic and abiotic conditions: a stirred flow-through
774 reactor study. Journal of Environmental Radioactivity 138: 38-49.

775 Gil-García C., Rigol A., Vidal M., 2009. New best estimates for radionuclide solid–liquid
776 distribution coefficients in soils, Part 1: radiostrontium and radiocaesium. Journal of
777 Environmental Radioactivity 100: 690-696.

778 Grigaliūnienė D., Poškas R., Kilda R., Jouhara H., Poškas P., 2020. Modeling radionuclide
779 migration from activated metallic waste disposal in a generic geological repository in
780 Lithuania. Nuclear Engineering and Design 370: 110885.

781 Huet S., Bouvier A., Poursat M.-A., Jolivet E., 2004. Accuracy of estimators, confidence
782 intervals and tests. Statistical Tools for Nonlinear Regression: A Practical Guide With S-
783 PLUS and R Examples. Springer Verlag, New York. https://doi.org/10.1007/b97288.

784 IAEA, 2009. Quantification of Radionuclide Transfer in Terrestrial and Freshwater
785 Environments for Radiological Assessments. Report IAEA-TECDOC-1616. International
786 Atomic Energy Agency, Vienna.

787 Ilina S.M., Marang L., Lourino-Cabana B., Eyrolle F., Boyer P., Coppin F., Sivry Y. Gélabert
788 A., Benedetti M.F., 2020. Solid/liquid ratios of trace elements and radionuclides during a
789 Nuclear Power Plant liquid discharge in the Seine River: Field measurements vs geochemical
790 modeling. Journal of Environmental Radioactivity 220-221: 106317.

791 Jackson M., 1962. Interlayering of expansible layer silicates in soils by chemical weathering.
792 Clays and clay minerals 11: 29-46.

793 Jagercikova M., Cornu S., Le Bas C., Evrard O., 2015. Vertical distributions of 137Cs in
794 soils: a meta-analysis. Journal of Soils and Sediments 15: 81-95.

795 Jarvis N.J., Taylor A., Larsbo M., Etana A., Rosén K., 2010. Modelling the effects of
796 bioturbation on the re-distribution of 137Cs in an undisturbed grassland soil. European
797 Journal of Soil Science 61: 24-34.

798 Klement A.W. Jr, 1965. Radioactive fallout phenomena and mechanisms. Health Physics 11:
799 1265-1274.

800 Konoplev A, Bulgakov A, Hilton J, Comans R, Popov V., 1997. Long-term kinetics of
801 radiocesium fixation by soils. In: G. Desmet et al. (Eds), Freshwater and Estuarine
802 Radioecology, Elsevier, pp. 173-182.

803 Kurikami H., Malins A., Takeishi M., Saito K., Iijima K., 2017. Coupling the advection-
804 dispersion equation with fully kinetic reversible/irreversible sorption terms to model
805 radiocesium soil profiles in Fukushima Prefecture. Journal of Environmental Radioactivity
806 171: 99-109.

807 Limousin G., Gaudet J.P., Charlet L., Szenknect S., Barthès V., Krimissa M., 2007. Sorption
808 isotherms: A review on physical bases, modeling and measurement. Applied Geochemistry
809 22: 249-275.

810 Maes A., Cremers A., 1986. Highly selective ion exchange in clay minerals and zeolites. In:
811 Geochemical Processes at Mineral Surfaces, Chapter 13, pp 254-295. ACS Symposium Series
812 Vol. 323. https://doi.org/10.1021/bk-1987-0323.ch013.

813 Maraqa M.A., Wallace R.B., Voice T.C., 1999. Effects of residence time and degree of water
814 saturation on sorption nonequilibrium parameters. Journal of Contaminant Hydrology 36: 53-
815 72.

816 Martin-Garin A., Van Cappellen P., Charlet L., 2003. Aqueous cadmium uptake by calcite: a
817 stirred flow-through reactor study. Geochimica et Cosmochimica Acta 67: 2763-2774.

818 Mazet P., 2008. Influence of transient flow on the mobility of strontium in unsaturated sand
819 columns (in french). PhD thesis, Université Joseph Fourier, Grenoble.

820 Medved' I., Černý R., 2019. Modeling of radionuclide transport in porous media: A review of
821 recent studies. Journal of Nuclear Materials 526: 151765.

822 Mishra S., Sahoo S.K., Bossew P., Sorimachi A., Tokonami S., 2018. Reprint of "Vertical
823 migration of radio-caesium derived from the Fukushima Dai-ichi Nuclear Power Plant
824 accident in undisturbed soils of grassland and forest". Journal of Geochemical Exploration
825 184: 271-295. https://doi.org/10.1016/j.gexplo.2016.07.027

826 Missana T., Benedicto A., García-Gutiérrez M., Alonso U., 2014a. Modeling cesium retention
827 onto Na-, K-and Ca-smectite: Effects of ionic strength, exchange and competing cations on
828 the determination of selectivity coefficients. Geochimica et Cosmochimica Acta 128: 266-
829 277.

830 Missana T., García-Gutiérrez M., Alonso U., 2004. Kinetics and irreversibility of cesium and
831 uranium sorption onto bentonite colloids in a deep granitic environment. Applied Clay
832 Science 26: 137-150.

833 Missana T., García-Gutiérrez M., Benedicto A., Ayora C., De-Pourcq K., 2014b. Modelling
834 of Cs sorption in natural mixed-clays and the effects of ion competition. Applied
835 Geochemistry 49: 95-102.

836 Montes M.L., Silva L.M.S., Sá C.S.A., Runco J., Taylor M.A., Desimoni J., 2013. Inventories
837 and concentration profiles of 137Cs in undisturbed soils in the northeast of Buenos Aires
838 Province, Argentina. Journal of Environmental Radioactivity 116: 133-140.

839 Murota K., Saito T., Tanaka S., 2016. Desorption kinetics of cesium from Fukushima soils.
840 Journal of Environmental Radioactivity 153: 134-140.

841 Nakamaru Y., Ishikawa N., Tagami K., Uchida S., 2007. Role of soil organic matter in the
842 mobility of radiocesium in agricultural soils common in Japan. Colloids and Surfaces A:
843 Physicochemical and Engineering Aspects 306: 111-117.

844 Nicoulaud-Gouin V., Garcia-Sanchez L., Giacalone M., Attard J.C., Martin-Garin A., Bois
845 F.Y., 2016. Identifiability of sorption parameters in stirred flow-through reactor experiments
846 and their identification with a Bayesian approach. Journal of Environmental Radioactivity
847 162-163: 328-339.

848 Okumura M., Kerisit S., Bourg I.C., Lammers L.N., Ikeda T., Sassi M., Rosso K.M., Machida
849 M. 2019. Radiocesium interaction with clay minerals: Theory and simulation advances Post–
850 Fukushima. Journal of Environmental Radioactivity 89: 135-145.

851 Ota M., Nagai H., Koarashi J., 2016. Modeling dynamics of 137Cs in forest surface
852 environments: Application to a contaminated forest site near Fukushima and assessment of
853 potential impacts of soil organic matter interactions. Science of The Total Environment 551-
854 552: 590-604.

855 Poinssot C., Baeyens B., Bradbury M.H., 1999. Experimental and modelling studies of
856 caesium sorption on illite. Geochimica et Cosmochimica Acta 63: 3217-3227.

857 Porro I., Newman M.E., Dunnivant F.M., 2000. Comparison of batch and column methods for
858 determining strontium distribution coefficients for unsaturated transport in basalt.
859 Environmental Science & Technology 34: 1679-1686.

860 R Core Team, 2021. R: A Language and Environment for Statistical Computing. R
861 Foundation for Statistical Computing, Vienna, Austria. https://www.R-project.org/

862 Rich C., Black W., 1964. Potasium exchange as affected by cation size, pH, and mineral
863 structure. Soil Science 97: 384-390.

Rigol A., Vidal M., Rauret G., 2002. An overview of the effect of organic matter on soil–radiocaesium interaction: implications in root uptake. Journal of Environmental Radioactivity 58: 191-216.

Rosén K., Öborn I., Lönsjö H., 1999. Migration of radiocaesium in Swedish soil profiles after the Chernobyl accident, 1987–1995. Journal of Environmental Radioactivity 46: 45-66.

Saiers J.E., Hornberger G.M., 1996. Migration of 137Cs through quartz sand: experimental results and modeling approaches. Journal of Contaminant Hydrology 22: 255-270.

Sardin M., Schweich D., Leij F.J., van Genuchten M.Th., 1991. Modeling the Nonequilibrium Transport of Linearly Interacting Solutes in Porous Media: A Review. Water Resources Research 27: 2287-2307.

Savoye S., Beaucaire C., Fayette A., Herbette M., Coelho D., 2012. Mobility of cesium through the callovo-oxfordian claystones under partially saturated conditions. Environmental Science & Technology 46: 2633-2641.

Sawhney B., 1972. Selective sorption and fixation of cations by clay minerals: a review. Clays and clay minerals 20: 93-100.

Schnaar G., Brusseau M.L., 2014. Nonideal Transport of Contaminants in Heterogeneous Porous Media: 11. Testing the Experiment Condition Dependency of the Continuous-Distribution Rate Model for Sorption-Desorption. Water, Air and Soil Pollution 225: 2136.

Schwertmann U., Taylor R.M., 1989. Iron oxides. In: Dixon, J.B. and Weed S.B. (Eds.), Minerals in Soil Environments, 2nd Edition, Soil Science Society of America, Inc., Madison, pp.379-438. https://doi.org/10.2136/sssabookser1.2ed.c8.

885 Seber G.A.F., Wild C.J., 1989. Nonlinear regression. John Wiley, New York.
886 https://doi.org/10.1002/0471725315.

887 Selim H., Mansell R., 1976. Analytical solution of the equation for transport of reactive
888 solutes through soils. Water Resources Research 12: 528-532.

889 Selim, H.M., Davidson J.M., Mansell R.S., 1976. Evaluation of a two-site adsorption–
890 desorption model for describing solute transport in soil. p. 444–448. In Proc. Summer
891 Computer Simulation Conf., Washington, DC. 12–14 July 1976. Simulation Councils, La
892 Jolla, CA.

893 Shenber M., Eriksson Å., 1993. Sorption behaviour of caesium in various soils. Journal of
894 Environmental Radioactivity 19: 41-51.

895 Siroux B., 2017. Interactions in a cesium, strontium/natural organic matter and soil clays
896 system. From decontamination to remediation (in french). PhD thesis. Université Sorbonne
897 Paris Cité. https://tel.archives-ouvertes.fr/tel-02083966

898 Siroux B., Latrille C., Beaucaire C., Petcut C., Tabarant M., Benedetti M.F., Reiller P.E.,
899 2021. On the use of a multi-site ion-exchange model to predictively simulate the adsorption
900 behaviour of strontium and caesium onto French agricultural soils, Applied Geochemistry
901 132, 105052. https://doi.org/10.1016/j.apgeochem.2021.105052.

902 Sparks D., Zelazny L., Martens D., 1980. Kinetics of potassium desorption in soil using
903 miscible displacement. Soil Science Society of America Journal 44: 1205-1208.

904 Sposito G., 1984. The surface chemistry of soils. Oxford University Press, New York.

905 Staunton S., Roubaud M., 1997. Adsorption of 137 Cs on montmorillonite and illite: effect of
906 charge compensating cation, ionic strength, concentration of Cs, K and fulvic acid. Clays and
907 clay minerals 45: 251-260.

908 Steinhauser G., Niisoe T., Harada K.H., Shozugawa K., Schneider S., Synal H.-A., Walther
909 C., Christl M., Nanba K., Ishikawa H., Koizumi A., 2015. Post-accident sporadic releases of
910 airborne radionuclides from the Fukushima Daiichi nuclear power plant site. Environmental
911 Science & Technology 49: 14028-14035.

912 Stewart G.W., 1987. Collinearity and least squares regression (with discussion). Statistical
913 Science 2: 68-100.

914 Strebl F., Gerzabek M., Bossew P., Kienzl K.., 1999 Distribution of radiocaesium in an
915 Austrian forest stand. Science of The Total Environment 226: 75-83.

916 Szenknect S., 2003. Radionuclides migration in the unsatured zone: experimental study and
917 modeling applied to the Chernobyl pilot site (in french). PhD thesis. Université Joseph
918 Fourier, Grenoble.

919 Szenknect S., Gaudet J.-P., Dewiere L., 2003. Evaluation of distribution coefficients for the
920 prediction of strontium and cesium migration in a natural sand at different water contents.
921 Journal de Physique IV (Proceedings) 107(1): 1279-1282.
922 https://doi.org/10.1051/jp4:20020534

923 Takahashi J., Onda Y., Hihara D., Tamura K., 2019. Six-year monitoring of the vertical
924 distribution of radiocesium in three forest soils after the Fukushima Dai-ichi Nuclear Power
925 Plant accident. Journal of Environmental Radioactivity 210: 105811.

926 Testoni R., Levizzari R., De Salve M., 2017. Coupling of unsaturated zone and saturated zone
927 in radionuclide transport simulations. Progress in Nuclear Energy 95: 84-95.

928 Toro J., Padilla I.Y., 2017. Spatial Distribution of Fate and Transport Parameters Using
929 CXTFIT in a Karstified Limestone Model. American Geophysical Union, Fall Meeting 2017,
930 abstract H51C-1288.

931 Toso J., Velasco R., 2001. Describing the observed vertical transport of radiocesium in
932 specific soils with three time-dependent models. Journal of Environmental Radioactivity 53:
933 133-144.

934 Soetaert, K., Petzoldt, T., Setzer, R.W., 2010. Solving differential equations in R: package
935 deSolve. J. Stat. Software 33 (9), 1-25. https://doi.org/10.18637/JSS.V033.I09.

936 Valcke E., Cremers A., 1994. Sorption-desorption dynamics of radiocaesium in organic
937 matter soils. Science of The Total Environment 157: 275-283.

938 Van Cappellen P., Qiu, L., 1997a. Biogenic silica dissolution in sediments of the Southern
939 Ocean. I. Solubility. Deep-Sea Res. Part II 1997; 44: 1109-1128.

940 Van Cappellen P, Qiu L., 1997b. Biogenic silica dissolution in sediments of the Southern
941 Ocean. II. Kinetics. Deep Sea Research Part II: Topical Studies in Oceanography 1997; 44:
942 1129-1149.

943 van Genuchten M.Th., Simunek J.J., Leij F.J., Toride N., Šejna M., 2012. STANMOD: Model
944 Use, Calibration, and Validation. Transactions of the ASAE 55:1353-1366.
945 https://doi.org/10.13031/2013.42247.

946 van Genuchten M.Th., Wagenet R.J., 1989. Two-Site/Two-Region Models for Pesticide
947 Transport and Degradation: Theoretical Development and Analytical Solutions. Soil Science
948 Society of America Journal 53: 1303-1310.

949 Wahlberg J., Fishman M.J., 1962. Adsorption of cesium on clay minerals. Geological Survey
950 Bulletin 1140-A, US Government Printing Office. https://doi.org/10.3133/b1140A.

951 Wang W.-Z., Brusseau M.L., Artiola J.F., 1998. Nonequilibrium and nonlinear sorption
952 during transport of cadmium, nickel, and strontium through subsurface soils. In: Jenne E.A.
953 (Ed.), Adsorption of Metals by Geomedia, Academic Press, pp. 427-443.
954 https://doi.org/10.1016/B978-012384245-9/50021-9.

955 Wendling L.A., Harsh J.B., Ward T.E., Palmer C.D., Hamilton M.A., Boyle J.S., Flury M.,
956 2005. Cesium desorption from illite as affected by exudates from rhizosphere bacteria.
957 Environmental Science & Technology 39: 4505-4512.

958 Yim M.-S., Simonson S.A., 2000. Performance assessment models for low level radioactive
959 waste disposal facilities: A review. Progress in Nuclear Energy 36: 1-38.

960 Zachara J.M., Smith S.C., Liu C., McKinley J.P., Serne R.J., Gassman P.L., 2002. Sorption of
961 Cs+ to micaceous subsurface sediments from the Hanford site, USA. Geochimica et
962 Cosmochimica Acta 66: 193-211.